Immunity-associated volatile emissions of β-ionone and nonanal propagate defence responses in neighbouring barley (*Hordeum vulgare*) plants

Alessandro Brambilla[1], Anna Sommer[1], Andrea Ghirardo[2], Marion Wenig[1], Claudia Knappe[1], Baris Weber[2], Melissa Amesmaier[1], Miriam Lenk[1], Jörg-Peter Schnitzler[2], A. Corina Vlot[1]*

[1]Helmholtz Zentrum München, Institute of Biochemical Plant Pathology, Neuherberg, Germany

[2]Helmholtz Zentrum München, Institute of Biochemical Plant Pathology, Research Unit Environmental Simulation, Neuherberg, Germany

*Author for correspondence: corina.vlot@helmholtz-muenchen.de

alessandro.brambilla@helmholtz-muenchen.de ORCID: 0000-0002-7228-1177
anna.sommer@helmholtz-muenchen.de
andrea.ghirardo@helmholtz-muenchen.de ORCID: 0000-0003-1973-4007
knappe@helmholtz-muenchen.de
marion.wenig@helmholtz-muenchen.de ORCID: 0000-0002-1389-2939
baris.weber@helmholtz-muenchen.de ORCID: 0000-0003-1179-4056
melissa@amesmaier.de
lenk.miriam@gmail.com
jp.schnitzler@helmholtz-muenchen.de ORCID: 0000-0002-9825-867X
corina.vlot@helmholtz-muenchen.de ORCID: 0000-0002-8146-6018

Date of submission: November 16th, 2021
Number of tables: 0
Number of figures: 6
Word count: 5271
Supplementary data: 5 Supplementary Tables, 2 Supplementary Figures

Running title:

Plant-to-plant defence propagation mediated by volatiles in barley

Abstract

Plants activate biochemical responses to combat stress. (Hemi-)biotrophic pathogens are fended off by systemic acquired resistance (SAR), a primed state allowing plants to respond faster and stronger upon subsequent infection. Here, we show that SAR-like defences in barley (*Hordeum vulgare*) are propagated between neighboring plants, which respond with enhanced resistance to the volatile cues from infected senders. The emissions of the sender plants contained 15 volatile organic compounds (VOCs) associated with infection. Two of these, β-ionone and nonanal, elicited resistance upon plant exposure. Whole genome transcriptomics analysis confirmed that inter-plant propagation of defence in barley is established as a form of priming. Although gene expression changes were more pronounced after challenge infection of the receiver plants with *Blumeria graminis* f. sp. *hordei*, differential gene expression in response to the volatile cues of the sender plants included an induction of *HISTONE DEACETYLASE 2* (*HvHDA2*) and priming of *TETRATRICOPEPTIDE REPEAT-LIKE superfamily protein* (*HvTPL*). Because *HvHDA2* and *HvTPL* transcript accumulation was also enhanced by exposure of barley to β-ionone and nonanal, our data identify both genes as possible defence/priming markers in barley. Our results further suggest that VOCs and plant-plant interactions are relevant for possible crop protection strategies priming defence responses in barley.

Highlight

Infected barley plants send airborne cues that are recognised as defence signals in conspecific neighbours. β-ionone and nonanal from the volatile blend of infected barley contribute to defence priming.

Keywords: barley, β-ionone, disease resistance, nonanal, plant immunity, powdery mildew, priming, systemic acquired resistance, volatile organic compound.

Abbreviations:

SAR	Systemic Acquired Resistance
VOCs	Volatile Organic Compound(s)
Psj	*Pseudomonas syringae* pv. *japonica*
Bgh	*Blumeria graminis* f. sp. *hordei*
PTP	Plant-to-plant
SA	Salicylic acid

RFU	Relative Fluorescence Unit
PDMS	Polydimethylsiloxane
Pip	Pipecolic acid
NHP	N-hydroxy pipecolic acid
LLP1	LEGUME LECTIN-like PROTEIN 1
AZI1	AZELAIC ACID INDUCED1
cfu	Colony Forming Unit
PR	*PATHOGENESIS-RELATED*
MeSA	Methyl salicylate
DIR1	DEFECTIVE IN INDUCED RESISTANCE1
GC-MS	Gas Chromatography-Mass Spectrometry
DAF-FM-DA	4-Amino-5-methylamino-2',7'-difluorofluorescein diacetate
ppbv	Parts per billion volume
TD-GC-MS	Thermal Desorption-Gas Chromatography-Mass Spectrometry
RI	Retention Index
GLV	Green Leaf Volatile(s)
HvEF1α	*Hordeum vulgare ELONGATION FACTOR 1α*
HvUBI	*Hordeum vulgare UBIQUITIN*
HvHDA2	*Hordeum vulgare HISTONE DEACETYLASE 2*
HvTPL	*Hordeum vulgare TETRATRICOPEPTIDE REPEAT (TPR)-like SUPERFAMILY PROTEIN*

Introduction

During their life cycle, plants experience a multitude of challenges, including stress imposed by their biotic and abiotic environment. On the one hand, plants are threatened by herbivorous insects and pathogenic microorganisms. On the other hand, adverse and changing climate conditions pose a stress on their own and additionally might alter the susceptibility of a plant to pests or diseases (Sangiorgio *et al*., 2020; Shahzad *et al*., 2021). As sessile organisms, plants evolved diverse biochemical responses to protect themselves from these threats (Spoel and Dong 2012). The activation of systemic acquired resistance (SAR) is a clear example of a biochemical strategy that plants have developed to fend off (hemi-)biotrophic microorganisms (Vlot *et al*., 2021). In SAR, an initial, local pathogen infection activates a cascade of reactions and the biosynthesis of several mobile defence cues that transmit the alert to distal parts of the plant (Gao *et al*., 2015; Vlot *et al*., 2021). Like priming, SAR activates a faster and stronger immune response to a subsequent pathogen attack (Westman *et al*., 2019).

Salicylic acid (SA) plays a fundamental role in SAR (Vlot *et al*., 2009), and its biosynthesis and recognition is crucial for inducing the expression of *PATHOGENESIS-RELATED* (*PR*) genes (Palmer *et al*., 2019). Nevertheless, other molecules are also involved in transmitting the immune signal to distal parts of the plant (Vlot *et al*., 2021; Gao *et al*., 2021). The methylated form of SA, methyl salicylate (MeSA), is one of several possible phloem-mobile molecules involved in systemic propagation of defence (Park *et al*., 2007; Park *et al*., 2009). Other important, potentially mobile molecules in the SAR network include the nonprotein amino acid pipecolic acid (Pip) and its bioactive derivative N-hydroxy pipecolic acid (NHP) as well as glycerol-3-phosphate and predicted lipid-transfer proteins, including AZELAIC ACID INDUCED1 (AZI1) and DEFECTIVE IN INDUCED RESISTANCE1 (DIR1) (Maldonado *et al.*, 2002; Chanda e*t* al., 2011; Návarová *et al*., 2012; Cecchini *et al*., 2015; Lim *et al*., 2016; Chen *et al*., 2018; Hartmann *et al*., 2018; Wang *et al*., 2018; Yildiz *et al*., 2021). In addition to being distributed through the phloem, volatile MeSA can also be dispersed through the air priming defence responses within and between plant canopies (Baldwin *et al*., 2006; Baldwin 2010). Beside this well-studied defence cue (Baldwin and Schultz 1983), we have recently shown the importance of monoterpenes as airborne molecules able to induce defence responses in distal plant parts during SAR (Riedlmeier *et al*., 2017).

Volatile organic compounds (VOCs) are low-molecular-weight compounds that easily evaporate at room temperature (Mofikoya *et al*., 2019). Plants produce volatiles constitutively or following biotic or abiotic stimuli (Loreto and Schnitzler 2010; Brilli *et al*., 2019). According to many studies (e.g., Baldwin and Schultz 1983; Piesik *et al*., 2013; Liu and Brettell, 2019; Markovic *et al*., 2019),

following the attack of an insect or the inoculation of a microbial pathogen, plants in the vicinity of their affected neighbours respond with enhanced/primed defences to future insect/pathogen attack. Riedlmeier and collaborators (2017) showed that VOCs emitted by SAR-induced plants are recognised as defence cues in plants that are in the vicinity. Specifically, trials on the model plant *Arabidopsis thaliana* infected with *Pseudomonas syringae* pv. *tomato* (*Pst*) expressing the effector *AvrRpm1*, revealed that monoterpenes, including α-pinene, β-pinene, and camphene play a central role as infochemicals.

Plant-to-plant (PTP) interaction is a phenomenon through which plants transfer information to each other (Baldwin and Schultz 1983). Trials on different plant species demonstrated that PTP interaction can occur between plants of the same or different species (Riedlmeier *et al*., 2017; Markovic *et al*., 2019; Ninkovic *et al*., 2019; Moreno *et al*., 2020; Frank *et al*., 2021). As plants face a threat caused by either biotic or abiotic stress, they emit a blend of VOCs in the air. These compounds can be intercepted by neighbouring plants that benefit by having more time to promptly activate a response to the change that may be harming them as well (Erb, 2018; Bouwmeester *et al*., 2019; Brilli *et al*., 2019). The mechanisms through which plant parts that are distant from the site of inoculation, perceive and process airborne cues remains unclear (Bouwmeester *et al*., 2019). Nevertheless, recent findings suggest the involvement of LEGUME LECTIN-LIKE PROTEIN 1 (LLP1) in signalling events downstream of volatile infochemicals leading to the establishment of SAR (Wenig *et al*., 2019). In plants that receive airborne cues from SAR-induced sender plants, LLP1 further drives a positive feedback loop with Pip and glycerol-3-phosphate to stimulate VOC biosynthesis and emission, potentially supporting the generation of a wave of plant-derived volatile defence cues moving between neighbouring plants (Wenig *et al*., 2019).

So far, molecular mechanisms associated with SAR have been uncovered mainly in the dicotyledonous *Arabidopsis* model system. In contrast, we know little about SAR-related processes in monocots, including cereals such as barley and wheat that are staple foods of the human population. Systemic immune responses have been observed in monocots, including maize, banana, wheat, and barley (Balmer *et al*., 2013; Yang *et al*., 2013; Wu *et al*., 2013; Dey *et al*., 2014). In barley, local infection with *Pseudomonas syringae* pv. *japonica* (*Psj*) enhances resistance in systemic tissues against different pathogens (Lenk *et al*., 2018; Dey *et al*., 2014). In this work, we set out to explore the potential role of VOCs in barley systemic immunity. We show that barley plants can sense airborne cues originating from infected neighbours, leading to enhanced defences in the receiver plant. Using a combination of gas chromatography-mass spectrometry (GC-MS), RNA-sequencing, and plant physiological analyses, we identified two VOCs that contribute to PTP

interaction in barley. Taken together, the results provide strong evidence that PTP interaction may be relevant to the induction of defence responses in barley and highlight the role of apocarotenoids and fatty acid-derivatives in their role as infochemicals.

Materials and methods

Plants and growth conditions

Barley seeds (*Hordeum vulgare* L., cultivar Golden Promise) were sterilised in a 1.2% (v:v) sodium hypochlorite solution for three minutes on a rotating shaker at a speed of 26 inversions per minute. Afterwards, the seeds were rinsed with sterile water for 10 minutes on the same shaker. This was repeated three times before sowing the seeds in normal potting soil (Einheits Erde; Classic Profisubstrat, Germany). Plants were grown in a climate chamber with 14/10 h light/dark conditions (light intensity: ca. 100 µmol cm^{-2} s^{-1} of maximum incident photosynthetically active quantum flux density (PPFD) levels at plant canopy) and temperatures of 20/16 °C, respectively. Three-week-old plants were used for all experiments.

Pathogen propagation and infection experiments

Pseudomonas syringae pv. *japonica* (*Psj*; strain LMG5659, LMG collection of the Belgian Coordinated Collections of Microorganisms) was propagated as described (Dey *et al*., 2014). To induce infection-associated VOC emissions, 10 plants per pot were inoculated with 10^8 colony forming units (cfu) of *Psj* in 10 mM $MgCl_2$ supplemented with 0.01 % Tween 20 (v:v) by spraying the plants until drop-off. Corresponding mock/control treatments were performed with 10 mM $MgCl_2$ supplemented with 0.01 % Tween-20 (Calbiochem, Merck KGaA, Darmstadt, Germany) (v:v). Afterwards, the plants were allowed to dry for 45 minutes prior to starting the experiments.

Blumeria graminis f. sp. *hordei* was propagated and inoculated as previously described at a density of 30 spores per mm^2 leaf area (Lenk *et al*., 2018, 2019). To this end, barley plants were treated in inoculation towers by shaking spores off of fully infected barley plants, which were used as the inoculum. To estimate the inoculation rate, spores per mm^2 were counted on glass slides, which were included in each inoculation procedure.

Plant-to-plant interaction experiments

Plants were grown and treated in galvanised steel pots (12 cm diameter; Socker, IKEA, Brunnthal, Germany) containing 10 sender plants per pot. Plants were spray-inoculated with 10^8 cfu ml^{-1} *Psj* or

with the corresponding mock/control treatment as described above, and each pot was placed at the centre of a glass vase (28 cm diameter x 59 cm height). Receiver plants were grown individually in pots (9 cm diameter x 18 cm height). Four receiver plants were placed in each vase with the 'sender' pots. In these experiments, *Psj*-infected plants were lightly tied together with a twine in order to avoid physical contact (and a possible propagation of the *Psj* infection) between sender and receiver plants. After three days, the receiver plants were removed from the vases and either infected with *Bgh* as described above and/or used to harvest leaf tissue for further analysis. To this end, 3 cm of leaf tissue was harvested from the second true leaf of the receiver plants immediately after the PTP exposure (T3, before infection) and 24 hours post *Bgh* inoculation (T4). At 7 days (d) post-inoculation (dpi), *Bgh* propagation in the inoculated plants was quantified in 4 leaf discs per plant, which were harvested from the second true leaf and stained with DAF-FM-DA as described below. Samples from one vase were considered technical replicates; independent biological replicates were performed at separate times at the frequencies indicated in the figure legends.

***Blumeria graminis* f. sp. *hordei* quantification (DAF-FM DA staining)**

Blumeria graminis f. sp. *hordei* infection levels were measured after staining the hyphae with 4-amino-5-methylamino-2',7'-difluorofluorescein diacetate (DAF-FM DA, Sigma Aldrich, Merck KGaA, Darmstadt, Germany) as described by Lenk *et al*. (2018, 2019). Stained leaf discs were distributed onto wells of 96-well plates, which had been filled with 1% (w:v) phytoagar (Carl Roth GmbH, Karlsruhe, Germany). DAF-FM DA fluorescence was excited with a 488 nm laser and detected using a 525/50 bandpass filter (Axio Observer.Z1; Zeiss, Jena, Germany). Fluorescence intensities were analysed using ZEN2 (Zeiss). In each experiment, all images were manually inspected for the presence of air bubbles in the wells, and the associated data were omitted from further analysis. For the remaining data points, fluorescence intensities were normalised to DAF-FM DA background fluorescence in leaf discs from untreated barley plants (Lenk *et al*., 2018; 2019).

VOC collection and analysis

Collection and analysis of VOCs were performed as described (Riedlmeier *et al*., 2017; Wenig *et al*., 2019). Plants were grown in galvanised steel pots, containing 10 plants each. Three week old plants were enclosed in conic glass cuvettes, each with ~31.7 L volume (height, base and top diameters: 45, 23.5, 18 cm, IKEA) 1 d prior to VOC sampling to allow acclimation to the new environment. Each cuvette was continuously flushed with 450 mL min^{-1} VOC-free synthetic air (Linde GmbH, Pullach, Germany) supplemented with CO_2 at a concentration of 410 parts per million by volume (ppmv). After acclimation, VOCs were collected in the cuvette outlet air on

polydimethylsiloxane-foam-adsorbent (PDMS, Gerstel GmbH, Mülheim an der Ruhr, Germany) for 8 hours (h) starting 1 h after the onset of light at a flow rate of 80 mL min^{-1} (Day 0 (D0) sample). The flow rates were regulated using mass flow controllers (MKS, Andover, USA), which were calibrated by a mass flow meter (ADM-3000, Agilent Technologies, Palo Alto, USA).

The next day, the plants were spray-inoculated with 10^8 cfu mL^{-1} of *Psj* or mock/control-treated as described above and kept in the cuvettes with an airflow of 450 mL min^{-1}. VOCs were collected as described for the D0 sample starting at 24 and 72 hpi (D2 and D4 samples), respectively. Background VOC emissions were measured using soil-filled pots, in which barley plants had been grown and subsequently had been removed 24 h before the enclosure of the pots in the cuvettes.

The VOCs on the PDMS cartridges were analysed by thermal desorption-gas chromatography-mass spectrometry (TD-GC-MS; TD, Gerstel; GC, 7890A and MS, 5975C both from Agilent Technologies, Palo Alto, CA, USA) following established procedures (Ghirardo *et al.*, 2012; 2016; 2020). The TD-GC-MS parameters followed those given in Ghirardo *et al.* (2020). Annotation was achieved by comparison of the mass spectra against libraries of reference spectra (NIST 11, Wiley 275) and non-isothermal Kovats retention indices (RI) found in literature (NIST Chemistry WebBook SRD 69, webbook.nist.gov). To quantify the VOC emissions, a calibration curve using six different concentrations of pure standard mixtures, independently created in triplicate, was performed. The standard mixtures contained the green leaf volatile (GLV) (*E*)-hex-3-en-1-ol (Sigma Aldrich, Merck KGaA, Darmstadt, Germany), the monoterpenes α-pinene and β-pinene (Carl Roth GmbH, Karlsruhe, Germany), the oxygenated monoterpenoids linalool (Carl Roth GmbH) and bornyl acetate (Sigma Aldrich, Merck KGaA, Darmstadt, Germany), the benzenoid MeSA (Fluka, Honeywell International Inc, Charlotte, North Carolina, USA), and the sesquiterpenes β-caryophyllene (Carl Roth GmbH) and α-humulene (Sigma Aldrich). The recorded MS signals were linear (r^2 = .986–.9993) for the range of 0–900 pmol, which covered the sampled VOC concentrations. Volatiles that were not included in the standard mixture were quantified using calculated response factors (Kreuzwieser *et al.*, 2014) with an absolute uncertainty of <8% (Ghirardo *et al.*, 2020). Each sample and calibration point contained the same amount of internal standard (860 pmol of δ-2-carene) and the respective peak areas were used for data normalization (Ghirardo *et al.*, 2016). To determine aboveground total plant VOC emissions, the means of peak areas detected in 15 blanks were subtracted from those obtained using plant samples. Finally, fluxes (emission rates) of VOC were calculated on leaf area basis (pmol m^{-2} s^{-1}) (Ghirardo *et al.*, 2011; Birami *et al.*, 2021). The projected leaf area (la) was derived from dry weight (dw) measurements performed as described below and estimated using the ratios of la:dw obtained in pre-experiments

under identical experimental conditions. In these experiments, we determined the la of the above-ground parts of 16 barley plants by taking pictures of their leaves on a scanner and calculating the leaf area (pixels/cm) with the open-source picture editor ImageJ (imagej.nih.gov). The leaves were dried at 60 °C for 48 h to obtain dry weight. Finally, la was estimated with a conversion factor as in Supplementary Table S1.

Exposure experiments

Pots with four three-week-old barley plants each were placed in 5.5 L air-tight glass desiccator as described (Riedlmeier *et al*., 2017). Pieces of 9 cm^2 filter paper (Whatman, Sigma Aldrich, Merck KGaA, Darmstadt, Germany) were used to apply the VOC treatments as described below and situated on the bottom of a glass dish, which was fitted between the plants at the centre of the pots. For the treatments, different concentrations of nonanal or β-ionone were diluted in hexane. Subsequently, plants were exposed to final air concentrations of 35, 55 or 115 parts per billion by volume (ppbv) of nonanal or 50, 75 or 150 ppbv of β-ionone; the same volume of hexane was applied as the corresponding mock/control treatment. The plants were exposed to the treatments for three consecutive days, during which the desiccators were opened once every 24 h to exchange the air and repeat the treatment (Riedlmeier *et al*., 2017). After three days, the plants were removed from the desiccators and infected with *Bgh* as described above. Leaf tissue for qRT-PCR analysis was harvested from the plants immediately after the exposure (T3, before infection) and 24 hours post *Bgh* inoculation (T4). *Bgh* propagation was quantified at 7 dpi as described above.

RNA-Sequencing

Leaf samples of 3 cm were collected from the distal part of the second true leaf of receiver plants in PTP interaction experiments as described above; each sample contained 4 leaf segments from 4 different receiver plants. RNA was isolated as described below. Transcript accumulation was analysed by RNA-sequencing (RNA-seq) at Novogene (Novogene Co., Ltd., United Kingdom). A total amount of one μg RNA per sample was used as input material. Sequencing libraries were generated using NEBNext® UltraTM RNA Library Prep Kit for Illumina® (NEB, USA) and barcode sequences for indexing were added to each sample/library as follows: mRNA was purified from total RNA using poly-T oligo-attached magnetic beads. Fragmentation was carried out using divalent cations under elevated temperature in NEBNext First Strand Synthesis Reaction Buffer (5X). First strand cDNA was synthesised using random hexamer primer and M-MuLV Reverse Transcriptase (RNase H-). Second strand cDNA synthesis was subsequently performed using DNA Polymerase I and RNase H. The clustering of the index-coded samples was performed on a cBot

Cluster Generation System using PE Cluster Kit cBot-HS (Illumina) according to the manufacturer's instructions.

The library preparations were sequenced on an Illumina platform and paired-end reads were generated. Reference genome and gene model annotation files were downloaded from the IPK Gatersleben (Monat *et al*., 2019). Paired-end clean reads were mapped to the MorexV2 reference genome using HISAT2 software (Monat *et al*., 2019). In total 512, 313, 920 sequences were read with an average of 42,692,826 reads per sample. Of that number, 478,313,528 reads were mapped to the reference genome with an average of 39,859,460 reads per sample. The following analysis was performed with R (R Development Core Team, 2020). Analysis of DEGs was done utilizing DESeq2 (Love *et al*., 2014), genes were considered significant DEGs with an FDR-adjusted p-value <0.05. The analysis for enriched GO terms among the DEGs was performed utilizing topGO (Alexa and Rahnenführer, 2020). GO analysis was performed separately on each DEG group (see below) with all DEGs per group as input data. Statistically significant enriched GO terms were determined using the Kolmogorov-Smirnov test (Ackermann and Strimmer, 2009) based on the "weight01" algorithm of topGO. Visualisation was performed with "ggplot2" (Wickham, 2016), including the packages "Gridextra" (Auguie, 2017), "ggVenn" (Yan, 2021), "ggpubr" (Kassambara, 2020) and "ggprism" (Dawson, 2021).

RNA isolation and qRT-PCR analysis

RNA isolation was carried out using Tri-Reagent according to the manufacturer's instructions (Sigma, Deisenhofen, Germany). Oligo(dT) (20-mer) and SuperScript II Reverse Transcriptase (Invitrogen, Hilden, Germany) were used to generate cDNA. qRT-PCR was performed using the primers listed in Supplementary Table S2. qPCR was performed with the SensiMix SYBR Low-ROX Kit (Meridian Life Sciences, Inc., Tennessee, USA) on a 7500 real-time PCR system (Applied Biosystems, Foster City, USA) as previously described (Breitenbach *et al*., 2014). Cycle threshold values (Ct) were quantified using the 7500 Fast System Software 1.3.1 (Applied Biosystems, Foster City, USA). Transcript accumulation of the genes-of-interest was normalised to that of the geometric mean of the two reference transcripts, *ELONGATION FACTOR1α* (*HvEF1α*; analysed with primers published in Dey *et al*., 2014) and *UBIQUITIN* (*HvUBI;* analysed with primers published in Ovesna *et al*., 2012), as described by Vandesompele *et al*. (2002) and Hellemans *et al*. (2007).

Statistical analysis

Data from *Bgh* quantification, GC-MS, and qRT-PCR analyses were evaluated using Graphpad Prism v8.1.1 (GraphPad Software, San Diego, US). Changes of volatile emissions were evaluated by two-way ANOVA with multiple comparisons versus the control groups Mock and D0 (Holm-Sidak method); data that were not normally distributed were evaluated with Kruskal–Wallis test. For *Bgh* quantification, unpaired Student *t*-tests were conducted. qRT-PCR data were normalised to mock T3 in case of PTP experiments and to hexane T3 in case of exposure experiments. Subsequently, qRT-PCR data from PTP experiments were evaluated with a one-way ANOVA with Tukey's multiple comparison test, each group versus Mock T3. qRT-PCR data from exposure experiments were evaluated with Student's *t* test.

Results

SAR induction enhances resistance against *Blumeria graminis* f. sp. *hordei* in neighbouring plants

To investigate whether monocots show an enhanced resistance when exposed to volatile emissions from infected conspecific neighbours, we inoculated barley sender plants with the systemic immunity-inducing pathogen *Psj* or with a corresponding mock control solution and placed them together with naïve receiver plants in open-top glass vases (Fig. 1a). After three days, the receiver plants were taken from the vases and inoculated with *Bgh*, propagation of which was monitored at 7 dpi. Differences in *Bgh* propagation on the leaves were visible by eye (Fig. 1b) and after fluorescent staining of the fungal hyphae with DAF-FM DA (Fig. 1c). Relative quantification of *Bgh*-associated DAF-FM-DA fluorescence revealed that *Bgh* propagation had been reduced (17 fold-change) on the leaves of receiver plants, which had been exposed to the infection-induced VOC emissions of *Psj*-inoculated senders as compared to the controls (Fig. 1d). With this result, we could confirm that *Psj*-infected barley plants emit VOCs that are recognised as airborne defence cues by neighbouring plants.

Characterization of SAR-induced VOC emission

To investigate which VOCs might play a role in PTP interaction in barley, we analysed the VOC emissions of *Psj*-infected and mock-treated plants. VOCs were sampled the day before the treatment (D0) and on day 2 (D2) and day 4 (D4) of the *Psj* infection or mock treatment, corresponding to 24 and 72 hpi, respectively.

In total, we could detect and identify 23 VOCs in the collected barley emissions. Of these, 8 compounds (toluene, ethyl benzene, p-cymene, benzyl alcohol, decanal, 1-pentadecene, calamenene and an unknown benzenoid) were constitutively emitted by the plants, with no difference between treatments (Fig 2a, Supplementary Table S3). Two compounds, α-methylstyrene and nonanal, were found in the emissions of untreated plants (D0) and significantly increased upon infection (Fig 2a and b). Notably, 13 VOCs were exclusively emitted following the *Psj* infection (Fig. 2a, Supplementary Table S3). Overall, barley plants displayed low emission rates; few compounds were emitted at >1 pmol m^{-2} s^{-1}, and most of these were constitutively emitted. Infection-induced VOCs were mostly emitted at an emission rate of <1 pmol m^{-2} s^{-1}. Within this last group, the VOCs with the highest emission rates were the alkene 1-undecene (~7 pmol m^{-2} s^{-1} on D2 and ~2 pmol m^{-2} s^{-1} on D4), the apocarotenoid β-ionone (~0.8 pmol m^{-2} s^{-1} on D4) and the fatty-acid derivative nonanal (~0.6 pmol m^{-2} s^{-1} on D2 and ~0.3 pmol m^{-2} s^{-1} on D4). Of these, nonanal and β-ionone were already known as infochemicals from other studies (Yi *et al*., 2009; Moreno *et al*., 2020; Paparella *et al*., 2021).

In further experiments described below, the effects of nonanal and β-ionone on barley immunity are assessed. Here, nonanal was emitted by un-infected plants and its emission responded to the *Psj* infection by a clear and significant increase (P = 0.004) on D2 (4-fold change) and D4 (5-fold change) as compared to healthy plants (Fig. 2b). By comparison, β-ionone was absent in the emission profile of healthy plants and became increasingly emitted after the inoculation of plants with *Psj* (Fig. 2c).

Gene regulation in receiver plants

To unravel possible molecular mechanisms underlying PTP-induced resistance in barley, we next analysed the genome-wide transcriptome of the receiver plants after 3 d of exposure to emissions of infected neighbours. Because induced resistance often is established as a form of priming, which is recognized at the molecular level only after a following challenge inoculation, we also analysed the transcriptome of the receiver plants at 24 h after the *Bgh* challenge inoculation. To this end, we performed the same experiment as above and exposed naïve receiver plants to the VOCs of *Psj*-inoculated or mock-treated barley senders. After 3 d, leaf material from the receiver plants was collected and analysed; data from this time point are labelled T3. Additional receiver plants were inoculated with *Bgh* and harvested 24 h later (T4) (Fig. 3a).

We detected a total of 5,150 differentially expressed genes (DEGs) by comparing relative transcript abundances in four different comparison groups (Fig. 3a). First, we analysed the influence of the

exposure on the transcriptome of receiver plants, comparing gene expression in receivers which were exposed to VOCs of *Psj*-infected senders to that in receivers which had been exposed to VOCs of mock-treated senders at T3 (Group I, *Psj* T3 – Mock T3, *Psj*-regulated genes, Fig. 3a-c). In the corresponding group I, 14 gene transcripts were significantly upregulated (Fig. 3b; Supplementary Table S4) and 4 were downregulated (Fig 3c; Supplementary Table S4). Strikingly, 13 of these DEGs represented genes, which could not be assigned to one of the chromosomes of the barley reference cultivar Morex (Monat *et al*., 2019; Supplementary Table S4). Five remaining DEGs with chromosome annotations included two genes with functional annotations: *HISTONE DEACETYLASE2* (*HvHDA2*) and *O-METHYLTRANSFERASE.* Here, we tested these as possible marker genes of PTP-induced defence responses. qRT-PCR analysis on samples from additional, biologically independent experiments confirmed the induction of *HvHDA2* and the reduction of *O-METHYLTRANSFERASE* transcript accumulation in receiver plants which shared their headspace with *Psj*-infected senders (Fig. 4a and b).

Next, we investigated a possible PTP-induced priming of gene expression changes. This was monitored by comparing transcript accumulation after *Bgh* inoculation of receivers (T4) that had been exposed to VOCs of *Psj*-infected plants as compared to receivers that had been exposed to VOCs of control-treated senders prior to the infection (Group IV, *Psj* T4 – Mock T4, primed genes, Fig. 3a-c). In the corresponding group IV, we detected 40 upregulated (Fig. 3b) and 61 downregulated transcripts (Fig. 3c), and thus a total of 101 primed gene expression changes. Primed DEGs included e.g., *HvHDA2*, whose PTP-induced upregulation in receiver plants (group I) was downregulated after *Bgh* infection of the same plants, but remained significantly higher than in the mock-treated controls, as confirmed in qRT-PCR analyses of an additional set of experiments (Fig. 4a). Consequently, *HvHDA2* appeared primed for enhanced expression by PTP interaction in the comparison group IV (Supplementary Table S4). Expression of the potentially defence-associated gene *TETRATRICOPEPTIDE REPEAT (TPR)-like SUPERFAMILY PROTEIN* (*HvTPL*) followed the more classical view on priming (Bernsdorff *et al*., 2016; Jung *et al*., 2009). Whereas *HvTPL* transcript accumulation appeared to be induced in receiver plants of emissions of *Psj*-infected senders in the RNA-seq data (group I, Supplementary Table S4), this could not be confirmed by qRT-PCR analysis (Fig. 4c). Thus, *HvTPL* was not robustly regulated in response to the emissions of *Psj*-infected senders or in response to a *Bgh* infection (groups II and III, Fig. 3a, Supplementary Table S4, below), while its transcript accumulation was significantly enhanced upon *Bgh* infection of PTP-primed plants (group IV, Fig. 3a, Supplementary Table S4). This was confirmed in qRT-PCR analyses of additional, biologically independent replicate experiments (Fig. 4c), suggesting *HvTPL* as a marker gene of PTP priming in barley. Strikingly, genes with functions in the light

reactions of photosynthesis were primed to be downregulated after inoculation of PTP-primed plants with *Bgh* (Group IV, Supplementary Table S4). This was confirmed for two of the corresponding genes (*PHOTOSYSTEM II D2 PROTEIN - 1* and *2*) in qRT-PCR analyses of samples from additional, biologically independent experiments (Fig. 4d and e). Taken together, our results suggest that the volatile emissions of *Psj*-infected barley senders prime defence responses at the transcriptional level in 'naïve' barley receivers.

Finally, we analysed the effect of the *Bgh* infection on gene expression, comparing T4 to T3 in each receiver group (Group II and III genes, Fig. 3a-c, Supplementary Table S4). Receivers of VOCs from mock-treated senders (Group II, Mock T4 – Mock T3, *Bgh*-regulated genes) displayed 2,636 upregulated and 2,157 downregulated genes in response to *Bgh* (Fig. 3a-c). Receivers of VOCs from *Psj*-infected senders (Group III, *Psj* T4 – *Psj* T3, *Bgh*-regulated/primed genes) displayed 1,018 upregulated and 1,016 downregulated genes (Fig. 3a-c). DEGs that were detected after infection in either group II or III included SA-associated genes, such as *PHENYLALANINE AMMONIA LYASE* and *PR* genes. Strikingly, such genes were neither induced (Group I) nor primed (Group IV) in receiver plants upon their exposure to the emissions of *Psj*-infected senders.

By comparing which DEGs were regulated in which comparison groups, only one DEG was specifically upregulated in the response of receiver plants to the volatile emissions of *Psj*-infected senders, while 3 genes were specifically downregulated in this group (Fig. 3b-c). *HvHDA2* constitutes one of 13 shared DEGs in the comparison groups I and IV, and is thus both induced and primed by PTP propagation of defence in barley (Figs. 3b and 4a). The comparison group T4 vs T3 mock (Group II) shared 869 upregulated and 841 downregulated DEGs with the group T4 vs T3 *Psj* (Group III); these DEGs were thus associated with the plant's response to *Bgh* (Fig. 3b-c). Further 1766 upregulated and 1290 downregulated DEGs were specific to the comparison group T4 vs T3 mock, and thus specifically associated with the response of 'naïve' barley to *Bgh*. These DEGs were not detected upon *Bgh* inoculation of PTP-primed plants. This shift might be caused in part by a general reduction of disease due to enhanced immunity of the primed plants, and in part by a priming-induced shift of transcriptional processes after infection. Taken together, we detected comparatively weak PTP-induced and –primed transcriptional responses in barley, which were accompanied by a comparatively strong shift in the transcriptional response of primed as compared to unprimed plants in response to a *Bgh* challenge infection. Thus, PTP priming markedly reduced and partially shifted the transcriptional response of barley to *Bgh* infection.

GO annotation of the DEGs revealed that genes which responded to PTP exposure to emissions of *Psj*-infected plants have functions in the chloroplast and mitochondrion as well as extracellularly (Fig. 3d; Supplementary Table S5). In particular the cellular compartment plastid was enriched in the GO annotations of DEGs that were associated with PTP-induced and primed responses (comparison groups I, III, and IV), whereas this was less pronounced in the plant's response to *Bgh* (comparison group II). The cellular compartment cytosol was moderately associated with the plant's response to *Bgh* (comparison group II and III) and this appeared fortified by PTP-induced priming (comparison group III and IV) (Fig. 3d). With respect to the biological process, the GO annotation was strongly enriched with genes associated with defence responses (comparison groups I, II, and III) but less in primed plants (comparison group IV) (Fig. 3e; Supplementary Table S5). In addition, after the *Bgh* infection (comparison group II) we observed changes in the expression of genes related to stress responses, and this was also significant in the primed sector (comparison group IV). In support of the gene expression and RT-qPCR data (Fig. 4d and e; Supplementary Table S4), genes related to the photosynthetic light reactions were less associated with *Bgh*-induced gene responses in primed plants (comparison group IV) as compared to any other comparison group.

Exposure of barley plants to nonanal and β-ionone enhances defence responses

To investigate a possible role of nonanal and β-ionone as signalling molecules able to induce defence in exposed plants, these VOCs were applied to barley plants at different concentrations. Interestingly, plants exposed to nonanal and β-ionone showed a decreased level of *Bgh* infection (up to 6-fold change with nonanal and 18-fold change with β-ionone) (Fig. 5a). Among the concentrations that were used to expose the plants, 35 and 55 ppbv nonanal and 50 and 75 ppbv β-ionone were most effective (Fig. 5b). Although all these concentrations induced a significant reduction of *Bgh* infection, nonanal was most effective at a concentration of 35 ppbv and β-ionone at 75 ppbv. As previously observed in *Arabidopsis* responding to different terpenes (Frank *et al.*, 2021; Riedlmeier *et al.*, 2017), higher concentrations did not induce a significant reduction in *Bgh* infection (Supplementary Fig. S2).

To compare the defence response to nonanal and β-ionone exposure with that triggered by PTP interaction, we analysed the transcript accumulation of 3 DEGs, which responded to or were primed by PTP interaction (Fig. 4a-c), in samples from exposure experiments. Similarly to its response to PTP interaction, *HvHDA2* was up-regulated at T3 in response to both nonanal and β-ionone (Fig. 5c and d). In the case of *HvTPL*, an up-regulation was expected at T4 but was observed in response to both nonanal and β-ionone at T3, maybe due to a stronger effect of the chemical exposure compared

to a natural PTP scenario (compare Figs. 5e and f to Fig. 4c). Finally, *O-METHYLRANSFERASE* followed the behaviour observed in receiver plants in PTP interaction experiments, with a down-regulation at T3 in nonanal- and β-ionone-treated plants as compared to the controls (Fig. 5g and h). Taken together, the data suggest that nonanal and β-ionone act as infochemicals in the volatile emissions of infected barley plants and are at least partially causative for immune propagation during PTP interaction in barley.

Discussion

Inter-plant interaction is a well-studied phenomenon. Plants have evolved strategies to interact with their neighbours that can depend on either air- or soil-borne cues (Zhao *et al*., 2018; Li *et al*., 2020b). Receiver plants respond to such cues by enhancing or priming their tolerance to a possible perturbance of the environment. Such perturbances can be of abiotic or biotic origin. In this work, we elucidated part of this biochemical scheme in barley responses to infection. .

Previously, we showed that *Arabidopsis* plants respond with enhanced resistance to the airborne cues emitted by infected neighbouring plants (Riedlmeier *et al*., 2017; Wenig *et al*., 2019; Frank *et al*., 2021). However, little is known about PTP interaction in barley and other monocots. Tolosa and co-workers (2019) demonstrated that VOCs emitted by the monocot *Melinis minutiflora*, commonly known as molasses grass, displayed a repellent effect against the stemborer, *Chilo partellus*, in neighbouring maize plants. The same study elucidated that maize plants displayed enhanced resistance when exposed to molasses grass' constitutive VOC emission. In maize and rice, indole emissions are induced in response to infestation of the plants with insects (Erb *et al.*, 2015; Zhuang *et al.*, 2012). In maize, indole emissions induced by *Spodoptera littoralis* are believed to prime herbivore resistance in infested and neighbouring plants (Erb *et al*., 2015). Ye and co-workers (2020) further validated the role of indole in priming defence signalling in dicotyledonous *Camellia sinensis* (tea) plants. Work published by Li and colleagues (2020c) elucidated the effectiveness of VOCs emitted by monocotyledonous Chinese chive (*Allium tuberosum*) against *Fusarium oxysporum* f. sp. *cubense*, the causal agent of Panama disease, in banana plantations. These studies consolidate the presence of defence-related PTP interaction events in monocots and their ability in reducing disease caused by insect pests or microorganisms in the field.

Studies on barley by Glinwood *et al*. (2009) investigated the function of VOCs emitted from different barley cultivars in attracting ladybirds as an effective strategy in controlling phloem-feeding aphids. Also, Jud and co-workers (2018) characterised barley VOC emissions following

benzothiadiazole (BTH) treatment through proton transfer reaction time-of-fight mass spectrometry (PTR-ToF-MS). This last study confirms that barley is a low-emitting plant species and that VOCs such as methanethiol, monoterpenes, and green leaf volatiles, including hexenal isomers, are emitted after a BTH treatment.

Our results suggest that a barley-PTP system with *Psj*-infected sender plants can dramatically reduce a subsequent *Bgh* infection in receiver plants (Fig. 1). After the inoculation with *Psj*, the relative abundance of 15 VOCs changed in the volatile blend that was emitted by barley (Fig. 2). Among these compounds, we characterised alkenes, aldehydes, ketones, aromatic compounds, diterpenes and apocarotenoids. In detail, most of these compounds are known secondary metabolites that are emitted by plants after different types of stresses (Cellini *et al*., 2021). 1-Undecene is an alkene that is also found in *Farfugium japonicum* essential oils and is a known plant metabolite (Kim *et al*., 2008). Yi and co-workers (2009) demonstrated that exposure of lima bean (*Phaseolus lunatus*) to nonanal increases the transcript accumulation of the defence-associated *PR2* gene in the exposed plants. 2-Undecanone is a ketone that is found naturally in banana, guava and other plant species (Kamal *et al*., 2019). Finally, another structural group of VOCs which we detected in the emissions of *Psj*-inoculated plants are apocarotenoids, including α-ionene, dehydro-β-ionone, α,β-dihydro-β-ionone, β-ionone, β-ionone-epoxide, β-cyclocitral, and dihydroactinidiolide. These compounds originate from the oxidative cleavage of carotenoids, which are C40 isoprenoids synthesised in plastids (Rodriguez-Concepcion et al, 2018). Murata *et al*. (2020), but also Paparella and co-workers (2021) highlight the biological role(s) of these compounds, in plant stress responses, growth and herbivore resistance. Some of the compounds are already known as infochemicals: β-ionone has been proven to have repellent effects against the crucifer leaf beatle (*Phyllotreta cruciferae*) (Wei *et al*. 2011) and silverleaf whiteflies (*Bemisia tabaci*) (Cáceres *et al*., 2016) in *Arabidopsis* plants over expressing *CAROTENOID CLEAVAGE DIOXYGENASE1* (*CCD1*), which is involved in the synthesis of apocarotenoids. Dihydroactinidiolide occurs naturally in several plant species (Shumbe *et al*., 2014) and originates from the degradation of β-ionone. β-Cyclocitral is a VOC common in several plant species (Felemban *et al*., 2019) and has been shown to affect lateral root development and to induce resistance against salt (Dickinson *et al*., 2019) and photo-oxidative stress (Ramel *et al*., 2012). Together, our results further confirm the importance of apocarotenoids as infochemicals and demonstrate their role in barley immune responses and PTP interaction.

In this work, we further studied if defence responses in neighbouring plants responding to the characterised VOCs in the emissions of *Psj*-infected barley were induced or primed. In order to test

this, we analysed PTP-induced gene expression changes in PTP receivers before a *Bgh* challenge inoculation and primed changes after *Bgh* inoculation (Fig. 3). One of the most notable changes in the receivers of emissions from *Psj*-infected plants was a marked shift in the number and nature of DEGs that were associated with a subsequent *Bgh* infection (compare groups III to II in Fig. 3). We further detected a higher number or primed DEGs (group IV) as compared to DEGs that were induced by the exposure of receivers to *Psj*-induced emissions (group I) (Fig. 3). Although we cannot exclude a reduction of *Bgh*-associated gene expression changes in primed as compared to unprimed plants due to compromised progression of the *Bgh* infection upon priming, we propose that the quantitative and, in particular, the qualitative shift in the *Bgh*-induced transcriptional profile in group III as compared to group II (Fig. 3) was related to an overall primed status of the receiver plant. In *Arabidopsis*, priming events, including transcriptional and metabolic reprogramming, hence a boosted activation of defences after future pathogen attack, can be triggered by SAR-associated molecules, including Aza, Pip and NHP (Jung *et al*., 2009; Návarová *et al*., 2012; Yildiz *et al*., 2021; Zeier 2021). Of these, we previously demonstrated that exogenous application of Pip primes reactive oxygen species accumulation and enhanced resistance against *Bgh* in barley (Lenk *et al*., 2019). Similarly, colonization of barley roots with the endophytic fungus *Serendipita indica* (formerly *Piriformospora indica*) primes immune responses in barley (Waller *et al*., 2005; Molitor *et al*., 2011). In the latter interaction, 8 DEGs were detected in leaf tissues of *S. indica*-colonised barley plants, while 41 *Bgh*-induced DEGs were primed by the same interaction (Molitor *et al*., 2011). Comparable to our observation, *S. indica*-induced priming was associated with a marked shift in transcriptional and metabolic changes after infection of the plants with *Bgh*. Together, our data suggest that PTP interaction-induced disease resistance in barley is established as a form of priming.

Strikingly, a noticeable number of DEG gene products are located in the ribosome and plastids (Fig. 3) highlighting the role of these organelles in plant-microbe interaction and in plant defence mechanisms in general (Lu and Yao, 2018; Kretschmer *et al*., 2020; Yang *et al*., 2021). Specifically, photosynthesis-related genes are primed for down-regulation after the challenge of PTP-primed plants with *Bgh* (Fig. 3). This is in line with findings of Molitor and co-workers (2011), who observed an overrepresentation of photosynthesis-related transcripts, which were down-regulated by *Bgh* at 24 hpi in barley leaves. These collective data from barley further support data from *Arabidopsis*, which show that photosynthesis and respiration rates are reduced in the systemic, primed tissues of SAR-induced plants (Bernsdorff *et al*., 2016). The reduction in net photosynthesis in primed plants, hence the reduced production of assimilates, is considered by many as an indirect cost of priming (Molitor *et al*., 2011; Douma *et al*., 2017). Our data further

confirm this hypothesis with reduced expression of genes that are associated with photosynthetic light reactions, in particular among the primed group IV genes (Fig. 3).

Bruce *et al*., (2007) discussed possible epigenetic changes in plants that are associated with priming. Specifically, DNA methylation and histone modifications are likely to enable a longer lasting primed status in the plant compared to the accumulation of metabolites (Jaskiewicz *et al*., 2011; Conrath *et al*., 2015; Li *et al*., 2020d). Interestingly, our results showed a PTP-induced upregulation of *HvHDA2* in plants that received *Psj*-induced VOC emissions (Fig. 4). This suggests a possible epigenetic-driven primed status in plants that were in the vicinity of *Psj*-infected plants. In wheat, *HISTONE DEACETYLASE 2* was identified as a negative regulator of defence responses against *Blumeria graminis* f. sp. *tritici* (Zhi *et al*., 2020). Similarly, in rice the overexpression of HD2 type histone deacetylase *OsHDT701* enhances rice susceptibility to the biotrophic pathogen *Magnaporthe oryzae* and the hemibiotrophic pathogen *Xanthomonas oryzae* pv. *oryzae* (Ding *et al*., 2012). In our work, after the challenge of primed plants with *Bgh*, the expression of *HvHDA2* was downregulated compared to that in the same plants before their inoculation with *Bgh* (Fig. 4). Thus, it is conceivable that *HvHDA2* contributes to the establishment of PTP priming, but not to the execution of the subsequent primed defence response.

Concomitantly, the expression of *HvTPL* was primed, i.e. upregulated only after *Bgh* inoculation of receivers of *Psj*-induced emissions (Fig. 4). . Tetraricopeptide repeats (TPR) are protein-protein interaction modules contained in many proteins. In *Arabidopsis*, TPR motif-containing proteins are involved in responses to hormones, including ethylene, cytokinins, auxins and gibberellins (Schapire *et al*., 2006). In plants, TPR-motifs are further involved in substrate recognition and/or in the generation of active multiprotein complexes thus, often playing roles in vital cellular processes (Cerveny *et al*., 2012). In rice, for example, TPR-containing proteins have been reported to regulate mRNA metabolism (Goebl and Yanagida, 1991). In addition, such TPR proteins or the multiprotein complexes they induce are involved in rice immunity against *Magnaporthe oryzae* and *Xanthomonas oryzae* pv *oryza* (Goebl and Yanagida, 1991; Zhou *et al*., 2018). Zhou and co-workers (2021) demonstrated that TPR-containing proteins in tomato, *Solanum lycopersicum*, are involved in responses to the biotic stress caused by necrotrophic fungi. Similarly to *HvTPL* in response to *Bgh* (Fig. 4), *SlTPR2* is up-regulated after challenge infection of tomato with *Botrytis cinerea*, and this might be associated with immunity. Thus, our collective data suggest that TPR-containing proteins, including *HvTPL*, play important roles in plant immunity and priming.

Exposure of barley plants to nonanal or β-ionone, which are both induced in the emissions of barley after inoculation of the plants with *Psj* (Fig. 2), enhanced the resistance of the plants against *Bgh*

(Fig. 5). After exposing barley plants to different concentrations of nonanal and β-ionone, we observed that the most effective concentrations with our experimental setup were 35 ppbv for nonanal and 75 ppbv for β-ionone, respectively. Good results were also obtained with 55 ppbv nonanal and 50 ppbv β-ionone. Higher concentrations of these compounds did not elicit defence in the exposed plants (Supplementary Fig. S2), suggesting possible negative feedback mechanisms taking effect if the system (i.e. barley) is over-stimulated (Rosenkranz *et al*., 2021). Similar to terpene-induced defence in *Arabidopsis*, the concentrations of nonanal and β-ionone which were used in the exposure experiments, were in an estimated >1000-fold higher range than what was measured in the emissions of *Psj*-inoculated barley (Frank *et al*., 2021; Riedlmeier *et al*., 2017). This supports other findings that plants in a natural context likely respond to VOC blends rather than to individual compounds, and that such compounds consequently are needed in considerably higher concentrations to elicit a response on their own (reviewed in Rosenkranz *et al*., 2021). Nevertheless, both of the exposure treatments induced the transcript accumulation of *HvHDA2* and *HvTPL*. In addition to confirming the potential role of these genes in defence, these data suggest that nonanal and β-ionone are among the causative VOCs promoting PTP propagation of immunity in barley.

In summary, our study shows that *Psj*-infected barley plants emit airborne cues (Fig. 6). These cues are subsequently recognised by receiver plants, which results in priming of defence responses to promptly react to a subsequent *Bgh* infection. Nonanal and β-ionone might play a central role in PTP interaction by inducing or priming the up-regulation of defence-related genes such as *HvHDA2* and *HvTPL* and by down-regulating *O-METHYLTRANSFERASE*. Earlier studies on PTP interaction showed the benefits of introducing VOC-emitting plants in agricultural fields (Pickett and Khan, 2016; Brilli *et al*., 2019). Similarly, intercropping barley with companion plants that are naturally emitting nonanal or β-ionone, could help in reducing *Bgh* infections and associated yield losses. Alternatively, recent studies demonstrated that the inclusion of VOC-based plant protection products in disease management programmes can reduce the input of chemical pesticides (Brilli *et al*., 2019; Ricciardi *et al*., 2021). Such crop protection strategies are likely to promote human health, to preserve natural ecosystems, and to avoid pesticide resistance in fields (Coelho, 2009).

In conclusion, our findings elucidate a possible role of VOCs in PTP propagation of immunity in the cereal crop barley. If and how this can be integrated into new crop protection strategies for this and other crop species will be subject to further investigation.

Data availability

The data from this study are available from the corresponding author, A. Corina Vlot, upon request.

Acknowledgements

We thank Prof. Dr. Wilfried Schwab (Technical University Munich, Germany) for helpful discussions. This project was funded in part by the DFG as part of SFB924 (project B06 to ACV).

Supplementary Materials

Supplementary Table S1 Determination of conversion factor dry weight (dw) to projected leaf area

Supplementary Table S2 Primers used in this study

Supplementary Table S3 Volatile Organic Compounds characterised in the emissions of barley

Supplementary Table S4 Summary of RNA-seq anaysis

Supplementary Table S5 Statistics of top 10 GO terms per comparison group

Supplementary Figure S1 Heatmap of the up- and down-regulated genes of the group *Psj* T4 vs. Mock T4 compared to the other groups.

Supplementary Figure S2 Nonanal and β-ionone do not enhance barley resistance against *Bgh* when applied at higher concentrations.

Author contributions

ACV conceived the project and acquired funding, AB, AG, MW, ML, JPS, and ACV conceived and planned experiments, AB, AG, MW, CK, BW, and MA executed experiments, AB, AS, AG, and ACV analysed the data, AB, AS, and ACV wrote the first draft of this manuscript, which was critically reviewed by all authors and edited by AG, ML, and JPS.

References

Ackermann M, Strimmer K. 2009. A general modular framework for gene set enrichment analysis. BMC Bioinformatics. 10, 47.

Alexa A, Rahnenführer J. 2020. Gene Set Enrichment Analysis with TopGO. https://bioconductor.riken.jp/packages/3.2/bioc/vignettes/topGO/inst/doc/topGO.pdf. Accessed August 2021.

Baldwin IT, Schultz JC. 1983. Rapid changes in tree leaf chemistry induced by damage: evidence for communication between plants. Science. 221, 277-279.

Baldwin IT, Halitschke R, Paschold A, Von Dahl CC, Preston CA. 2006. Volatile signaling in plant-plant interactions: "talking trees" in the genomics era. Science. 311, 812-815.

Baldwin IT. 2010. Plant volatiles. Current Biology 20, 392-397.

Balmer D, de Papajewski D, Planchamp C, Glauser G, Mauch-Mani B. 2013. Induced resistance in maize is based on organ-specific defence responses. The Plant Journal 74, 213-225.

Bernsdorff F, Döring AC, Gruner K, Schuck S, Bräutigam A, Zeier J. 2016. Pipecolic acid orchestrates plant systemic acquired resistance and defense priming via salicylic acid-dependent and -independent pathways. The Plant Cell 26, 102-129.

Birami B, Bamberger I, Ghirardo A, Grote R, Arneth A, Gaona-Colmán E, Nadal-Sala D, Ruehr N. 2021. Heatwave frequency and seedling death alter stress-specific emissions of volatile organic compounds in Aleppo pine. Oecologia doi: 10.1007/s00442-021-04905-y.

Bouwmeester H, Schuurink RC, Bleeker PM, Schiestl F. 2019. The role of volatiles in plant communication. The Plant Journal. 100, 892–907.

Brilli F, Loreto F, Baccelli I. 2019. Exploiting Plant Volatile Organic Compounds (VOCS) in agriculture to improve sustainable defense strategies and productivity of crops. Frontiers in Plant Science 10, 264.

Bruce TJA, Matthes MC, Napier Ja, Pickett JA. 2007. Stressful “memories” of plants: Evidence and possible mechanisms. Plant Science 173, 603-608.

Cáceres LA, Lakshminarayan S, Yeung KKC, McGarvey BD, Hannoufa A, Sumarah MW, Benitez X, Scott IM. 2016. Repellent and attractive effects of α-, β-, and dihdro-β-ionone to generalist and specialist herbivores. Journal of Chemical Ecology 42, 107-117.

Cecchini NM, Steffes K, Schläppi MR, Gifford AN, Greenberg JT. 2015. Arabidopsis AZI1 family proteins mediate signal mobilization for systemic defence priming. Nature Communications 6, 7658.

Cellini A, Spinelli F, Donati I, Ryu CM, Kloepper JW. 2021. Bacterial volatile compound-based tools for crop management and quality. Trends in Plant Science 26, 968-983.

Cerveny L, Straskova A, Dankova V, Hartlova A, Ceckova M, Staud F, Stullk J. 2021. Tetratricopeptide Repeat Motifs in the world of bacterial pathogens: role in virulence mechanisms. Infection and Immunity 81, 629-635.

Chanda B, Xia Y, Mandal MK, *et al.* 2011. Glycerol-3-phosphate is a critical mobile inducer of systemic immunity in plants. Nature Genetics 43, 421-427.

Coehlo S. 2009. European pesticide rules promote resistance, researchers warn. Science 323, 450.

Dawson C. 2021. Package 'ggprism' Title A 'Ggplot2' Extension Inspired by 'GraphPad Prism.' https://csdaw.github.io/ggprism/, https://github.com/csdaw/ggprism. Accessed August 2021.

Dey S, Wenig M, Langen G, *et al.* 2014. Bacteria-triggered systemic immunity in barley is associated with WRKY and ETHYLENE RESPONSIVE FACTORs but not with salicylic acid. Plant Physiology 166, 2133-2155.

Dickinson AJ, Lehner K, Mi J, Jia KP, Mijar M, Dinneny J, *et al*. 2019. β-Cyclocitral is a conserved root growth regulator. Proceedings of the National Academy of Sciences 116, 10563-10567.

Ding B, del Rosario Bellizzi M, Ning Y, Meyers BC, Wang GL. 2012. HDT701, a histone H4 deacetylase, negatively regulates plant innate immunity by modulating histone H4 acetylation of defense-related genes in rice. The Plant Cell 24, 3783-3794.

Douma JC, Vermeulen PJ, Poelman EH, Dicke M, Anten NPR. 2017. When does it pay off to prime for defense? A modeling analysis. The New Phytologist 216, 782-797.

Erb M. 2018. Volatiles as inducers and suppressors of plant defense and immunity-origins, specificity, perception and signaling. Current opinion in plant biology 44, 117-121.

Erb M, Veyrat N, Robert CAM, Xu H, Frey M, Ton J, Turlings TCJ. 2015. Indole is an essential herbivore-induced volatile priming signal in maize. Nature Communication 6, 6273.

Felemban A, Braguy J, Zurbriggen MD, Al-Babili S. 2019. Apocarotenoids involved in plant development and stress response. Frontiers in Plant Science 10, 1168.

Frank L, Wenig M, Ghirardo A, van der Krol A, Vlot AC, Schnitzler JP, Rosenkranz M. 2021. Isoprene and β-Caryophyllene confer plant resistance via different plant internal signalling pathways. Plant Cell and Environmen 44, 1151-1164.

Gao Q, Zhu S, Kachroo P, Kachroo A. 2015. Signal regulators of systemic acquired resistance. Frontiers in Plant Science 6, 228.

Gao H, Guo M, Song J, Ma Y, Xu Z. 2021. Signals in systemic acquired resistance of plants against microbial pathogens. Molecular Biology Reports 48, 3747-3759.

Glinwood R, Ahmed E, Qvarfordt E, Ninkovic V, Pettersson J. 2009. Airborne interactions between undamaged plants of different cultivars affect insect herbivores and natural enemies. Arthropod-Plant Interactions 3, 215–224.

Ghirardo A, Gutknecht J, Zimmer I, Brüggemann N, Schnitzler JP. 2011. Biogenic volatile organic compound and respiratory CO_2 emissions after ^{13}C-labeling: online tracing of C translocation dynamics in poplar plants. PLoS ONE 6, e17393.

Ghirardo A, Heller W, Fladung M, Schnitzler JP, Schroeder H. 2012. Function of defensive volatiles in Pedunculate oak (*Quercus Robur*) is tricked by the moth *Tortrix Viridana*. Plant, Cell & Environment 35, 2192-2207.

Ghirardo A, Lindstein F, Koch K, Buegger F, Schloter M, Albert A, Michelsen A, Winkler JB, Schnitzler JP, Rinnan R. 2020. Origin of volatile organic compound emissions from subarctic tundra under global warming. Global Change Biology 26, 1908-1925.

Ghirardo A, Xie J, Zheng X, *et al*. 2016. Urban stress-induced biogenic VOC emissions and SOA-forming potentials in Beijing. Atmospheric Chemistry and Physics 16, 2901–2920.

Goebl M, Yanagida M. 1991. The TPR snap helix: a novel protein repeat motif from mitosis to transcription. Trends in Biochemical Sciences 16, 173-177.

Hartmann M, Zeier T, Bernsdoff F, *et al*. 2018. Flavin monooxygenase-generated N-hydroxypipecolic acid is a critical element of plant systemic immunity. Cell 173, 456-469.

Hellemans J, Mortier G, Da Paepe A, Speleman F, Vandesompele J. 2007. qBase relative quantification framework and software for management and automated analysis of real-time quantitative PCR data. Genome Biology 8, R19.

Jaskiewicz M, Conrath U, Peterhänsel C. 2011. Chromatin modification acts as a memory for systemic acquired resistance in the plant stress response. EMBO Reports 12, 50-55.

Jud W, Winkler JB, Niederbacher B, Niederbacher S, Schnitzler JP. 2018. Volatilomics: a non-invasive technique for screening plant phenotypic traits. Plant Methods 14, 109.

Jung HW, Tschaplinski TJ, Wang L, Glazebrook J, Greenberg JT. 2009. Priming in systemic plant immunity. Science 324, 89-9.

Kamal AM, El-Tantawy ME, Haggag EG, Shukr MH, El-Garhy AMG, Lilthy RM. 2019. Chemical and biological analysis of essential oils and pectins of banana, cantaloupe peels, guava pulp and formulation of banana pectin gel. Journal of Pharmacognosy and Phytochemistry 8, 1808-1816.

Kassambara A. 2020. 'ggplot2' Based Publication Ready Plots [R Package Ggpubr Version 0.4.0]. https://CRAN.R-project.org/package=ggpubr. Accessed August 2021.

Kim JY, Oh TH, Kim BJ, Kim SS, Lee NH, Hyun CG. 2008. Chemical composition and anti-inflammatory effects of essential oil from *Farfugium japonicum* flower. Journal of Oleo Science 57, 623-628.

Kretschmer M, Damoo D, Djamei A, Kronstad J. 2020. Chloroplasts and plant immunity: where are the fungal effectors? Pathogens 9, 19.

Kreuzwieser J, Scheerer U, Kruse J, *et al*. 2014. The venus flytrap attracts insects by the release of volatile organic compounds. Journal of Experimental Botany 65, 755-766.

Lenk M, Wenig M, Bauer K, et al. 2019. Pipecolic acid is induced in barley upon infection and triggers immune responses associated with elevated nitric oxide accumulation. Molecular Plant-Microbe Interactions 32, 1303-1313.

Lenk M, Wenig M, Mengel F, Häußler F, Vlot AC. 2018. *Arabidopsis thaliana* immunity-related compounds modulate disease susceptibility in barley. Agronomy 8, 142.

Li S, Zhang J, Liu H, Liu N, Shen G, Zhuang H, Wu J. 2020a. Dodder-transmitted mobile signals prime host plants for enhanced salt tolerance. Journal of Experimental Botany 71, 1171-1184.

Li LL, Zhao HH, Kong CH. 2020b. (–)-Loliolide, the most ubiquitous lactone, is involved in barnyardgrass-induced rice allelopathy. Journal of Experimental Botany 71, 1540-1550.

Li Z, Wang T, He C, Cheng K, Zeng R, Song Y. 2020c. Control of Panama Disease of banana by intercropping with Chinese chive (*Allium Tuberosum* Rottler): cultivar differences. BMC Plant Biology 20, 432.

Li D, Liu R, Singh D, Yuan X, Kachroo P, Raina R. 2020d. JMJ14 encoded H3K4 demethylase modulates immune responses by regulating defence gene expression and pipecolic acid levels. The New Phytologist 225, 2108-2121.

Lim GH, Shine MB, de Lorenzo L, Yu K, Cui K, Navarre D, Hunt AG, Lee JY, Kachroo A, Kachroo P. 2016. Plasmodesmata localizing proteins regulate transport and signaling during systemic acquired immunity in plants. Cell Host and Microbe 19, 541-549.

Liu H, Brettell LE. 2019. Plant defense by VOC-induced microbial priming. Trends in Plant Science 24, 187-189.

Loreto F, Schnitzler JP. 2010. Abiotic stresses and induced BVOCs. Trends in plant science 15, 154-166.

Love MI, Huber W, Anders S. 2014. Moderated estimation of fold change and dispersion for RNA-Seq data with DESeq2. Genome Biology 15, 550.

Lu Y, Yao J. 2018. Chloroplasts at the crossroad of photosynthesis, pathogen infection and plant defense. International Journal of Molecular Sciences, 19, 3900.

Maldonado AM, Doerner P, Dixon RA, Lamb CJ, Cameron RK. 2002. A putative lipid transfer protein involved in systemic resistance signalling in Arabidopsis. Nature 419, 399-403.

Markovic D, Colzi I, Taiti C, Ray S, Scalone R, Ali JG, Mancuso S, Ninkovic V. 2019. Airborne signals synchronize the defenses of neighboring plants in response to touch. Journal of Experimental Botany 70, 691-700.

Mofikoya AO, Bui TNT, Kivimäenpää M, Holopainen JK, Himanen SJ, Blande JD. 2019. Foliar behaviour of biogenic semi-volatiles: potential applications in sustainable pest management. Arthropod-Plant Interactions 13, 193-212.

Molitor A, Zajic D, Voll LM, Pons-Kühnemann J, Samans B, Kogel K, Waller F. 2011. Barley leaf transcriptome and metabolite analysis reveals new aspects of compatibility and *Piriformora indica*-mediated systemic induced resistance to powdery mildew. Molecular Plant-Microbe Interactions 24, 1427–1439.

Monat C, Padmarasu S, Lux T *et al*. 2019. TRITEX: chromosome-scale sequence assembly of Triticeae genomes with open-source tools. Genome Biology 20, 284.

Moreno JC, Mi J, Alagoz Y, Al□Babili S. 2020. Plant apocarotenoids: from retrograde signaling to interspecific communication. The Plant Journal 105, 351-375.

Murata M, Kobayashi T, Seo S. 2020. α-Ionone, an apocarotenoid, induces plant resistance to western flower thrips, *Frankliniella occidentalis*, independently of jasmonic acid. Molecules 25, 17.

Návarová H, Bernsdorff F, Doring AC, Zeier J. 2012. Pipecolic acid, an endogenous mediator of defense amplification and priming, is a critical regulator of inducible plant immunity. The Plant Cell 24, 5123-5141.

Ninkovic V, Rensing M, Dahlin I, Markovic D. 2019. Who is my neighbor? Volatile cues in plant interactions. Plant Signaling and Behavior 14, 1559-2324.

Ovesna J, Kucera L, Vaculova K, Strymplova K, Svobodova I, Milella L. 2012. Validation of the *beta-amy1* transcription profiling assay and selection of reference genes suited for a RT-qPCR assay in developing barley caryopsis. PLoS One 7, e41886.

Palmer IA, Chen H, Chen J, Chang M, Li M, Liu F, Fu ZQ. 2019. Novel salicylic acid analogs induce a potent defense response in Arabidopsis. International Journal of Molecular Sciences 20, 3356.

Paparella A, Shaltiel-Harpaza L, Ibdah M. 2021. β-Ionone: its occurrence and biological function and metabolic engineering. Plants (Basel) 10, 754.

Park SW, Kaimoyo E, Kumar D, Mosher S, Klessig DF. 2007. Methyl salicylate is a critical mobile signal for plant systemic acquired resistance. Science 318, 113-116.

Park SW, Liu PP, Forouhar F, Vlot AC, Tong L, Tietjen K, Klessig DF. 2009. Use of a synthetic salicylic acid analog to investigate the roles of methyl salicylate and its esterases in plant disease resistance. Journal of Biological Chemistry 284, 7307-7317.

Pickett JA, Khan ZR. 2016. Plant volatile-mediated signalling and its application in agriculture: successes and challenges. The New Phytologist 212, 856-870.

Piesik DD, Jeske PM, Wenda-Piesik A, Delaney KJ, Weaver DK. 2013. Volatile induction of infected and neighbouring uninfected plants potentially influence attraction/repellence of a cereal herbivore. Journal of Applied Entomology 137, 296-309.

Ramel F, Birtic S, Cuiné S, Triantaphylidès C, Ravanat JL, Havaux M. 2012. Chemical quenching of singlet oxygen by carotenoids in plants. Plant Physiology 158, 1267-1278.

Ricciardi V, Marcianò D, Sarglozaei M, *et al*. 2021. From plant resistance response to the discovery of antimicrobial compounds: The role of volatile organic compounds (VOCs) in grapevine downy mildew infection. Plant Physiology and Biochemistry 160, 294-305.

Riedlmeier M, Ghirardo A, Wenig M, Knappe C, Koch K, Georgii E, Dey S, Parker JE, Schnitzler JP, Vlot AC. 2017. Monoterpenes support systemic acquired resistance within and between plants. The Plant Cell 29, 1440-1459.

Rodriguez-Concepcion M, Avalos J, Bonet ML *et al*. 2018. A global perspective on carotenoids: metabolism, biotechnology, and benefits for nutrition and health. Progress in Lipid Research 70, 62-93.

Rosenkranz M, Chen Y, Zhu P, Vlot AC. 2021. Volatile terpenes – mediators of plant-to-plant communication. The Plant Journal 108, 617-631.

Sangiorgio D, Cellini A, Donati I, Pastore C, Onofrietti C, Spinelli F. 2020. Facing climate change: application of microbial biostimulants to mitigate stress in horticultural crops. Agronomy 10, 794.

Schapire AL, Valpuesta V, Botella MA. 2006. TPR proteins in plant hormone signaling. Plant Signaling & Behavior 1, 229-230.

Shahzad A, Ullah S, Dar AA, Sardar MF, Mehmood T, Tufail MA, Shakoor A, Haris M. 2021. Nexus on climate change: agriculture and possible solution to cope future climate change stresses. Environmental Science and Pollution Research 28, 14211-14232.

Shumbe L, Bott R, Havaux M. 2014. Dihydroactinidiolide, a high light-induced β-carotene derivative that can regulate gene expression and photoacclimation in Arabidopsis. Molecular Plant 7, 1248-1251.

Spoel SH, Dong X. 2012. How do plants achieve immunity? Defence without specialized immune cells. Nature Reviews Immunology 12, 89-100.

Tolosa TA, Tamiru A, Midega CAO, et al. 2019. Molasses grass induces direct and indirect defense responses in neighbouring maize plants. Journal of Chemical Ecology 45, 982-992.

Vandesompele J, De Preter K, Pattyn F, Poppe B, Van Roy N, De Paepe A, Speleman F. 2002. Accurate normalization of real-time quantitative RT-PCR data by geometric averaging of multiple internal control genes. Genome Biology 3, research0034.1.

Vlot AC, Dempsey DMA, Klessig DF. 2009. Salicylic acid, a multifaceted hormone to combat disease. Annual Review of Phytopathology 47, 177-206.

Vlot AC, Sales JH, Lenk M, Bauer K, Brambilla A, Sommer A, Chen Y, Wenig M, Nayem S. 2020. Systemic propagation of immunity in plants. The New Phytologist 229, 1234–1250.

Wang KLC, Li H, Ecker JR. 2002. Ethylene biosynthesis and signaling networks. The Plant Cell 14, 131-151.

Waller F, Achatz B, Baltruschat H, et al. 2005. The endophytic fungus *Piriformospora indica* reprograms barley to salt-stress tolerance, disease resistance, and higher yield. Proceeding of the National Academy of Sciences of the United States of America 102, 13386-13391.

Wei S, Hannoufa A, Soroka J, Xu N, Li X, Zebarjadi A, Gruber M. 2011. Enhanced β-ionone emission in Arabidopsis over-expressing AtCCD1 reduces feeding damage in vivo by the crucifer flea beetle. Environmental Entomology 40, 1622–1630.

Wenig M, Ghirardo A, Sales JH, Pabst E, Breitenbach HH, Antritter F, Weber B, *et al*. 2019. Systemic acquired resistance networks amplify airborne defense cues. Nature Communications 10, 3813.

Westman SM, Kloth KJ, Hanson J, Ohlsson AB, Albrectsen BR. 2019. Defence priming in Arabidopsis – a meta-analysis. Scientific Reports 9, 13309.

Wu Y, Yi G, Peng X, Huang B, Liu E, Zhang J. 2013. Systemic acquired resistance in Cavendish banana induced by infection with an incompatible strain of *Fusarium oxysporum* f. sp. *cubense*. Journal of Plant Physiology 170, 1039-1046.

Yang F, Xiao K, Pan H, Liu J. 2021. Chloroplast: the emerging battlefield in plant–microbe interactions. Frontiers in Plant Science 12, 637853.

Yang Y, Zhao J, Liu P, Xing H, Li C, Wei C, Kang Z. 2013. Glycerol-3-phosphate metabolism in wheat contributes to systemic acquired resistance against *Puccinia striiformis* f. sp. *tritici*. PLoS ONE 8, e81756.

Ye M, Liu M, Erb M, Glauser G, Zhang J, Li X, Sun X. 2020. Indole primes defence signalling and increases herbivore resistance in tea plants. Plant, Cell & Environment 44, 1165-1177

Yi HS, Heil M, Adame-Álvarez RM, Ballhorn DJ, Ryu CM. 2009. Airborne induction and priming of plant defenses against a bacterial pathogen. Plant Physiology 151, 2152-2161.

Yildiz I, Mantz M, Hartmann M, et al. 2021. The mobile SAR signal N-hydroxypipecolic acid induces NPR1-dependent transcriptional reprogramming and immune priming. Plant Physiology 186, 1679-1705.

Zeier J. 2021. Metabolic regulation of systemic acquired resistance. Current Opinion in Plant Biology 62, 102050.

Zhao M, Cheng J, Guo B, Duan J, Che CT. 2018. Momilactone and related diterpenoids as potential agricultural chemicals. Journal of Agricultural and Food Chemistry 66, 7859-7872.

Zhi P, Kong L, Liu J, *et al*. 2020. Histone deacetylase TaHDT701 functions in TaHDA6-TaHOS15 complex to regulate wheat defense responses to *Blumeria graminis* f.sp. *tritici*. International Journal of Molecular Sciences 21, 2640.

Zhou C, Zhang L, Duan J, Miki B, Wu K. 2005. HISTONE DEACETYLASE19 is involved in jasmonic acid and ethylene signaling of pathogen response in Arabidopsis. The Plant Cell 17, 1196-1204.

Zhou X, Liao H, Chern M, *et al*. 2018. Loss of function of a rice TPR-domain RNA-binding protein confers broad-spectrum disease resistance. Proceedings of the National Academy of Sciences of the United States of America 115, 3174-3179.

Zhou X, Zheng Y, Cai Z, *et al*. 2021. Identification and functional analysis of Tomato TPR Gene Family. International Journal of Molecular Sciences 22, 758.

Zhuang X, Fiesselmann A, Zhao N, Chen H, Frey M, Chen F. 2012. Biosynthesis and emission of insect herbivory-induced volatile indole in rice. Phytochemistry 73, 15-22.

Figure legends

Figure 1 Plant-to-plant (PTP) propagation of defence in barley. (a) Set-up of a PTP experiment. Naïve receiver (R) plants were placed in open-top glass vases together with sender (S) plants, which were either mock-treated (Mock) or inoculated with *Pseudomonas syringae* pv. *japonica* /*Psj*). After 3 days, the receiver plants were inoculated with *Blumeria graminis* f. sp. *hordei* (*Bgh*). (b) *Bgh* on barley leaves. Pictures were taken at 7 dpi. (c) Fluorescence microscopy images of *Bgh* hyphae on leaf discs stained with DAF-FM-DA at 7 dpi. (d) Quantification of *Bgh* propagation in DAF-FM-DA stained leaf discs. *Bgh*-associated relative fluorescence units (RFU) were calculated by normalising the measured fluorescence values to those of uninfected controls. Bars represent average RFU values of 12 samples +/- standard error. Values are taken from a representative experiment. We repeated the experiment 12 times and obtained comparable results. **** = $P < 0.0001$ (unpaired *t* test).

Figure 2 Characterisation of VOC emissions in barley PTP experiments. (a) Heat map of the VOCs detected in the emissions of mock-treated (Mock) and *Psj*-inoculated plants at D0 (before treatment), D2 (24 hpi), and D4 (72 hpi). Darker colours indicate higher emission rates; black-coloured cells indicate out-of-range values (> 1). Each cell represents average values from 8 independent replicates. ° indicates tentatively identified compounds. (b,c) VOC emission rates of nonanal (b) and β–ionone (c) in mock-treated (Mock) and *Psj*-inoculated plants. Dashed lines separate timepoints before and after treatment. Bars represent average values of 8 independent replicates +/- standard error. * = $P < 0.05$; *** = $P < 0.0005$ (two-way ANOVA).

Figure 3 RNA-seq analysis of transcript accumulation in receiver plants in PTP experiments. Plants were either mock-treated or inoculated with *Psj*, and subsequently harvested at 3 dpi (T3) or inoculated with *Bgh* and harvested 1 day later (T4). (a) Timeline of the experiment. The RNA-seq data from two biologically independent replicate experiments were used to determine differentially expressed genes (DEGs) in four comparison groups (group definitions to the right of the timeline). (b,c) Venn diagrams of upregulated (b) and downregulated DEGs (c) in the different comparison groups. (d,e) GO-term enrichment in the categories cellular component (d) and biological process (e) among DEGs in the different comparison groups. Colours indicate *p*-value.

Figure 4 qRT-PCR validation of selected DEGs. Plants were either mock-treated or inoculated with *Psj*, and subsequently harvested at 3 dpi (T3) or inoculated with *Bgh* and harvested 1 day later (T4). Transcript accumulation of the indicated genes was analysed by qRT-PCR and normalised to that of

HvEF1α and *HvUBI*. Accumulation of transcripts is shown relative to that at T3 in mock-treated samples. Bars represent average values from 4 biologically independent experiments +/- standard error. * = P < 0.05; ** = P < 0.005; *** = P < 0.0005; **** = P < 0.0001 (one-way ANOVA, Tukey's multiple comparison test).

Figure 5 Exposure to nonanal and β-ionone enhances resistance in barley against *Bgh*. Plants were exposed to the indicated concentrations of nonanal or β-ionone (in hexane) or to a comparable amount of hexane as the mock control treatment. Three days later, leaves were either harvested (T3) or inoculated with *Bgh* and evaluated at 7 dpi. (a) *Bgh* on barley leaves; pictures were taken at 7 dpi. (b) Quantification of *Bgh* propagation in DAF-FM-DA stained leaf discs. *Bgh*-associated relative fluorescence units (RFU) were calculated by normalising the measured fluorescence values to those of uninfected controls. Bars represent average values of 12 samples +/- standard error. Values are taken from a representative experiment. We repeated the experiment 8 times and obtained comparable results. *** = P < 0.0005 (one-way ANOVA, Tukey's multiple comparison test). (c-h) qRT-PCR analysis of transcript accumulation of the indicated genes after exposure of barley to β-ionone (blue bars) and nonanal (yellow bars). Transcript levels were normalised to that of *HvEF1α* and *HvUBI* and are shown relative to those in hexane-treated samples (grey bars). Bars represent average values of 3 biologically independent experiments +/- standard error. * = P < 0.05; ** = P < 0.005; *** = P < 0.0005; **** = P < 0.0001 (unpaired *t* test).

Figure 6 Working model of plant-to-plant propagation of defence in barley. After the infection with *Pseudomonas syringae* pv. *japonica* (1), barley plants emit volatile organic compounds (2) that include nonanal and β-ionone. These chemicals are recognised as defence cues in barley plants that are in the vicinity (3). Similarly, exogenous application of nonanal and β-ionone (4) induces comparable responses in barley plants that are exposed to these compounds.

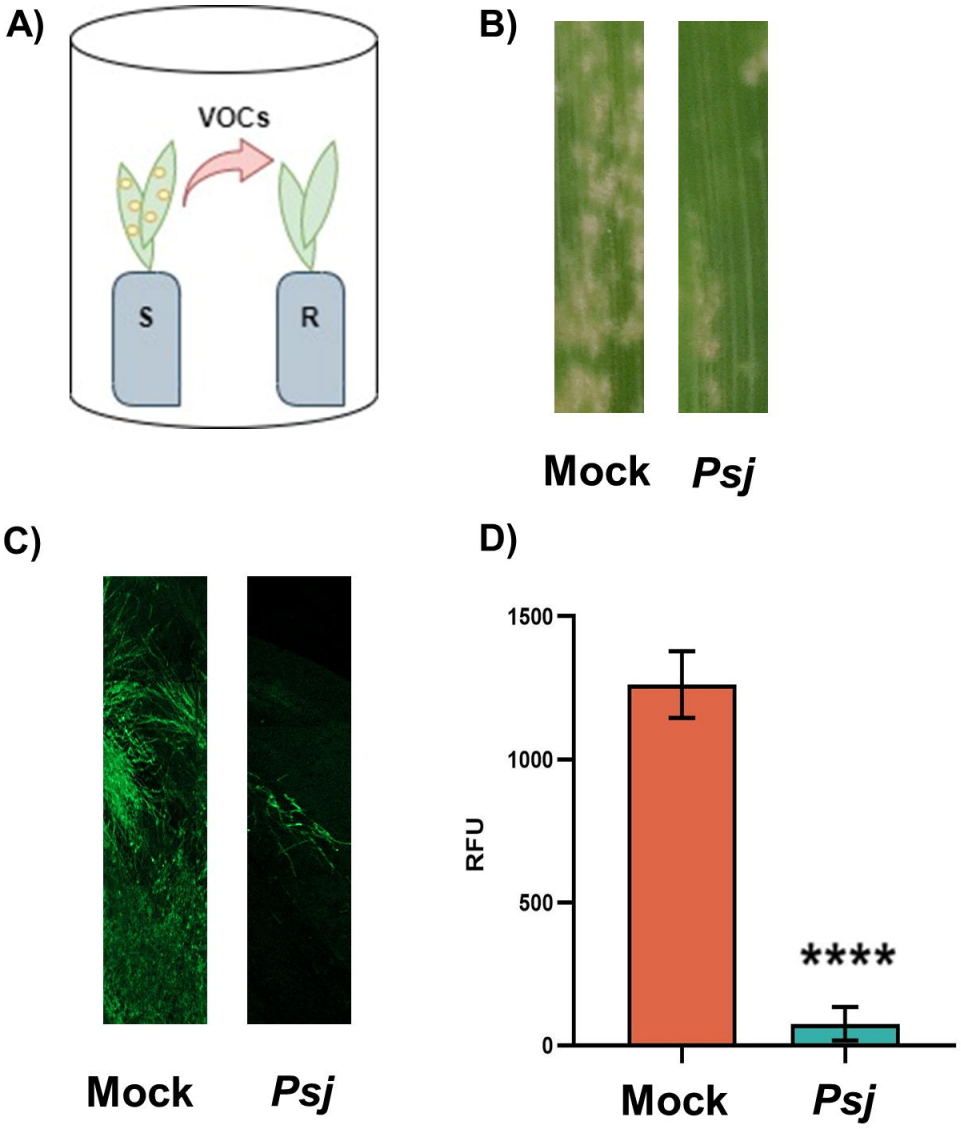

Figure 1 Plant-to-plant (PTP) propagation of defence in barley. (A) Set-up of a PTP experiment. Naïve receiver (R) plants were placed in open-top glass vases together with sender (S) plants, which were either mock-treated (Mock) or inoculated with *Pseudomonas syringae* pv. *japonica* /*Psj*). After 3 days, the receiver plants were inoculated with *Blumeria graminis* f. sp. *hordei* (*Bgh*). (B) *Bgh* on barley leaves. Pictures were taken at 7 dpi. (C) Fluorescence microscopy images of *Bgh* hyphae on leaf discs stained with DAF-FM-DA at 7 dpi. (D) Quantification of *Bgh* propagation in DAF-FM-DA stained leaf discs. *Bgh*-associated relative fluorescence units (RFU) were calculated by normalising the measured fluorescence values to those of uninfected controls. Bars represent average RFU values of 12 samples +/- standard error. Values are taken from a representative experiment. We repeated the experiment 12 times and obtained comparable results. **** = $P < 0.0001$ (unpaired *t* test).

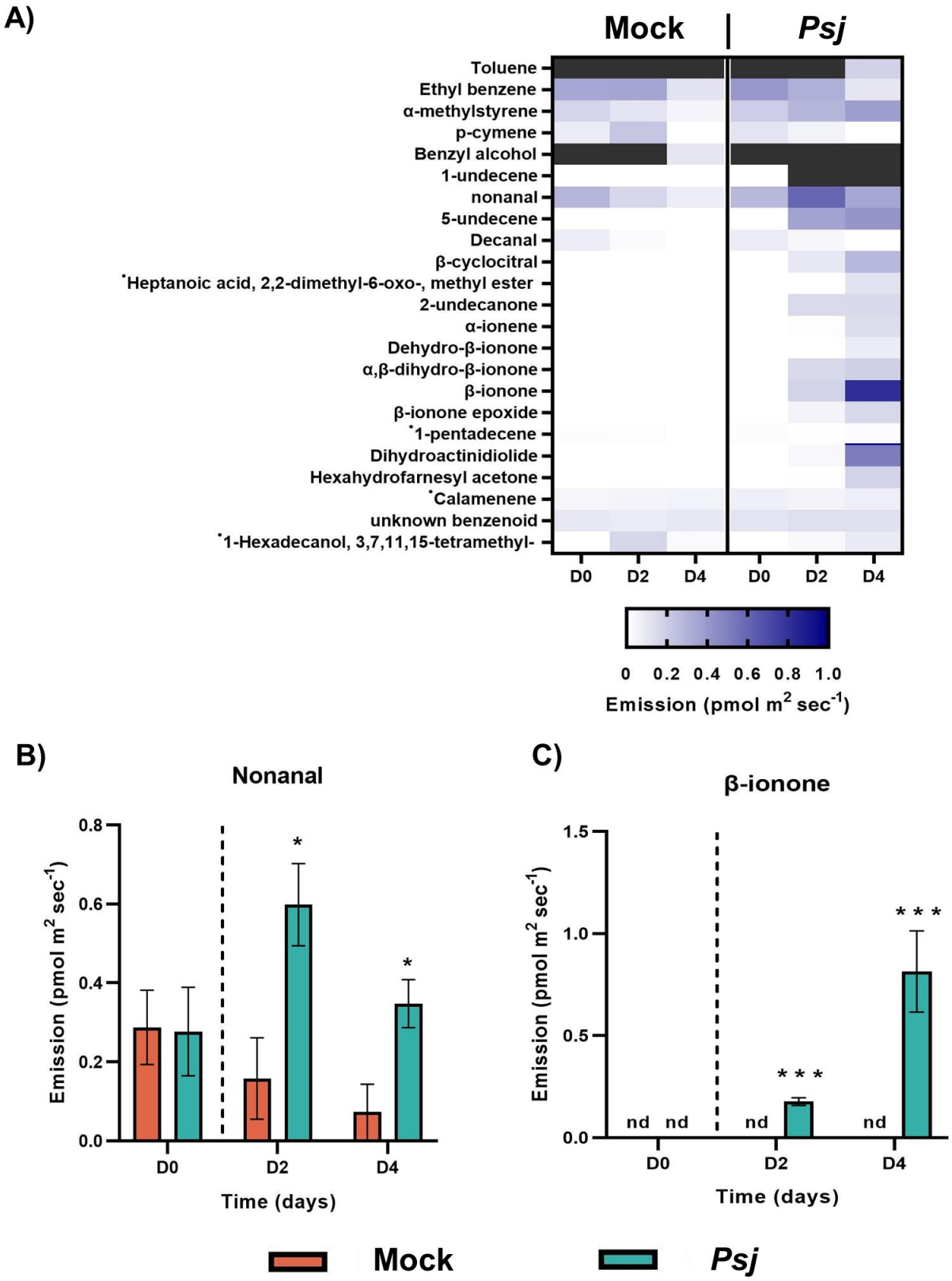

Figure 2 Characterisation of VOC emissions in barley PTP experiments. (A) Heat map of the VOCs detected in the emissions of mock-treated (Mock) and *Psj*-inoculated plants at D0 (before treatment), D2 (24 hpi), and D4 (72 hpi). Darker colours indicate higher emission rates; black-coloured cells indicate out-of-range values (> 1). Each cell represents average values from 8 independent replicates. ° indicates tentatively identified compounds. (B,C) VOC emission rates of nonanal (B) and β –ionone (C) in mock-treated (Mock) and *Psj*-inoculated plants. Dashed lines separate timepoints before and after treatment. Bars represent average values of 8 independent replicates +/- standard error. * = $P < 0.05$; *** = $P < 0.0005$ (two-way ANOVA).

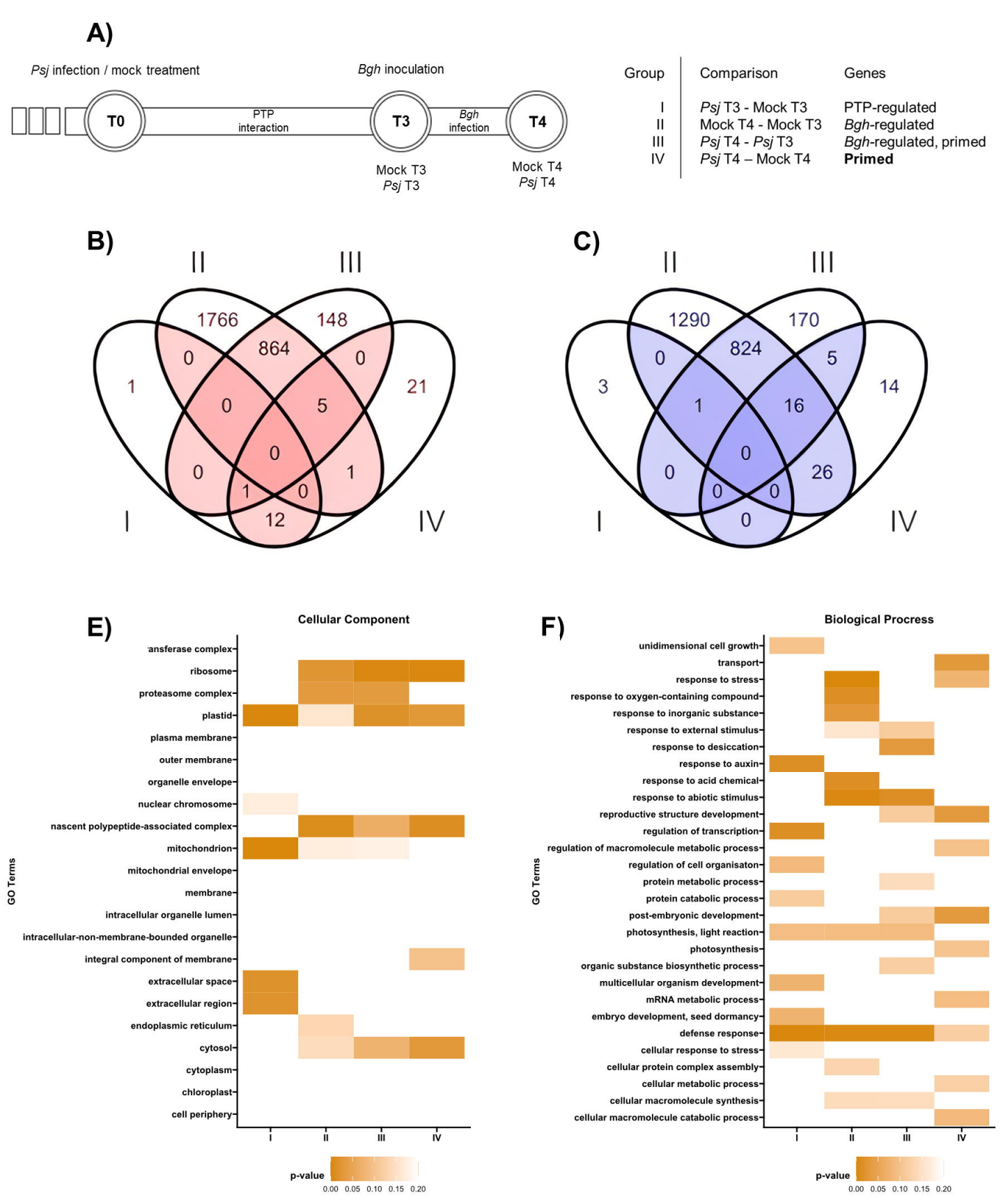

Figure 3 RNA-seq analysis of transcript accumulation in receiver plants in PTP experiments. Plants were either mock-treated or inoculated with *Psj*, and subsequently harvested at 3 dpi (T3) or inoculated with *Bgh* and harvested 1 day later (T4). (A) Timeline of the experiment. The RNA-seq data from two biologically independent replicate experiments were used to determine differentially expressed genes (DEGs) in four comparison groups (group definitions to the right of the timeline). (B,C) Venn diagrams of upregulated (B) and downregulated DEGs (C) in the different comparison groups. (D,E) GO-term enrichment in the categories cellular component (D) and biological process (E) among DEGs in the different comparison groups. Colours indicate *p*-value.

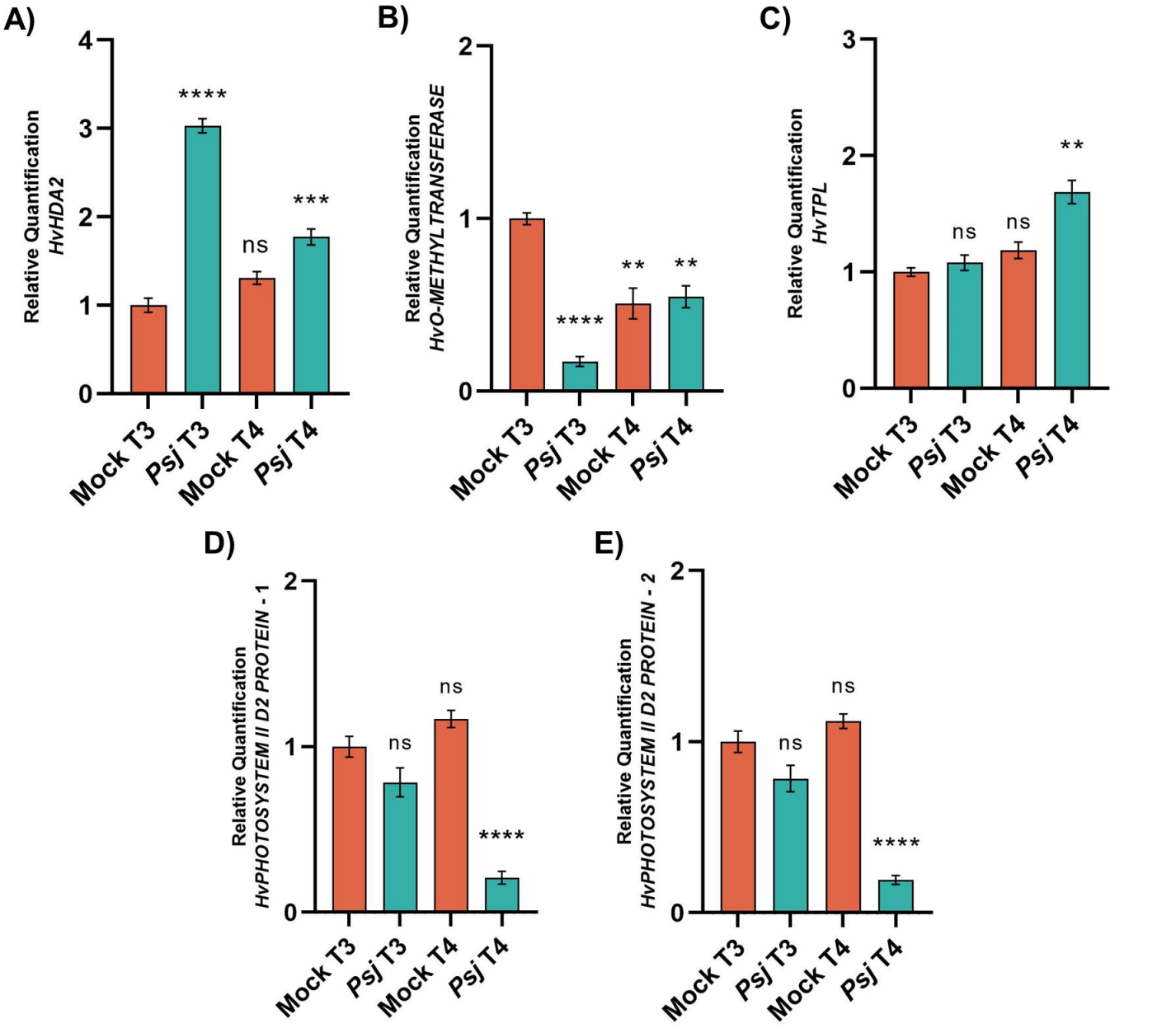

Figure 4 qRT-PCR validation of selected DEGs. Plants were either mock-treated or inoculated with *Psj*, and subsequently harvested at 3 dpi (T3) or inoculated with *Bgh* and harvested 1 day later (T4). Transcript accumulation of the indicated genes was analysed by qRT-PCR and normalised to that of *HvEF1α* and *HvUBI*. Accumulation of transcripts is shown relative to that at T3 in mock-treated samples. Bars represent average values from 4 biologically independent experiments +/- standard error. * = $P < 0.05$; ** = $P < 0.005$; *** = $P < 0.0005$; **** = $P < 0.0001$ (one-way ANOVA, Tukey's multiple comparison test).

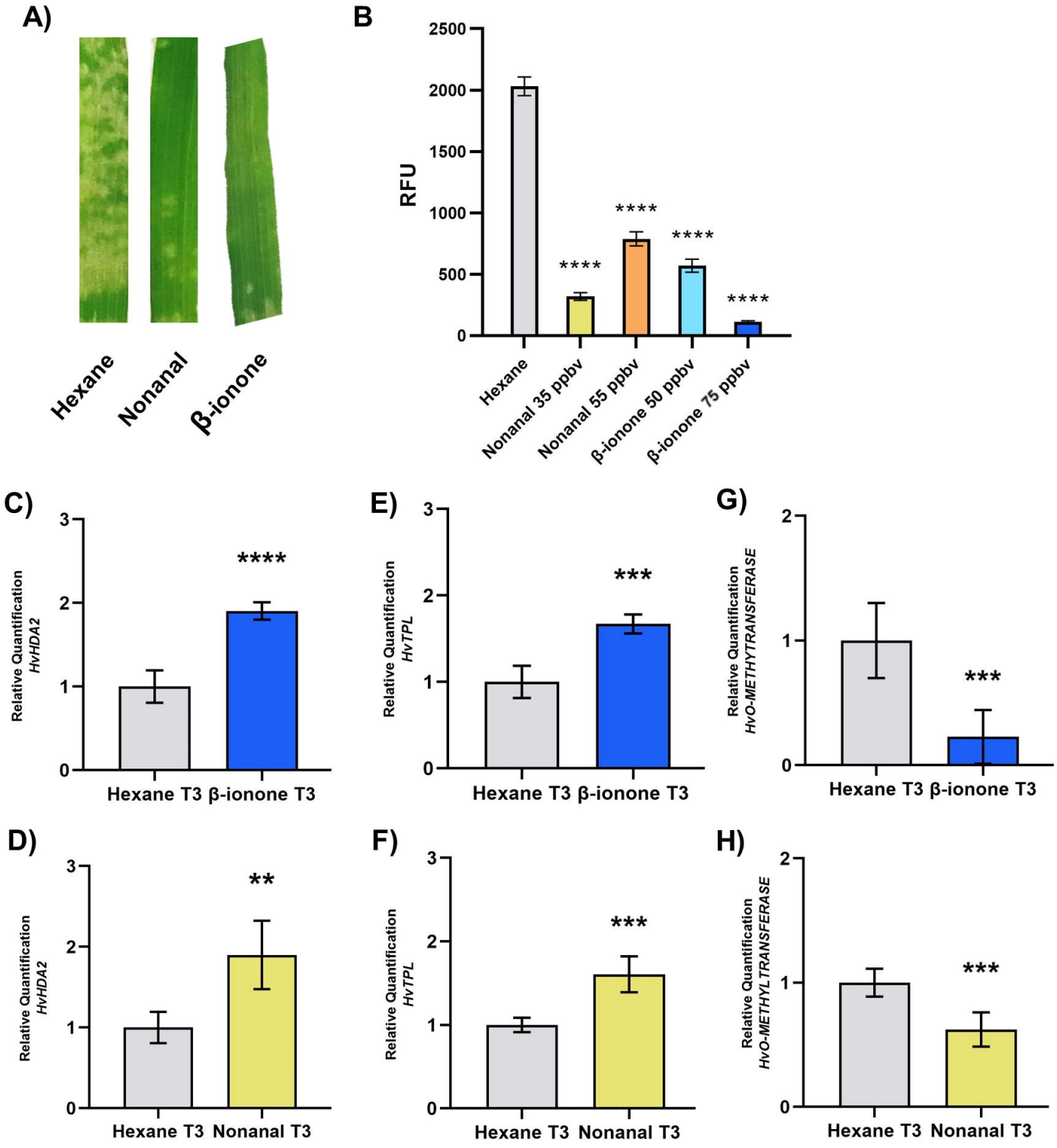

Figure 5 Exposure to nonanal and β-ionone enhances resistance in barley against *Bgh*. Plant were exposed to the indicated concentrations of nonanal or β-ionone (in hexane) or to a comparable amount of hexane as the mock control treatment. Three days later, leaves were either harvested (T3) or inoculated with *Bgh* and evaluated at 7 dpi. (A) *Bgh* on barley leaves; pictures were taken at 7 dpi. (B) Quantification of *Bgh* propagation in DAF-FM-DA stained leaf discs. *Bgh*-associated relative fluorescence units (RFU) were calculated by normalising the measured fluorescence values to those of uninfected controls. Bars represent average values of 12 samples +/- standard error. Values are taken from a representative experiment. We repeated the experiment 5 times and obtained comparable results. *** = $P < 0.0005$ (one-way ANOVA, Tukey's multiple comparison test). (C-H) qRT-PCR analysis of transcript accumulation of the indicated genes after exposure of barley to β-ionone (blue bars) and nonanal (yellow bars). Transcript levels were normalised to that of *HvEF1α* and *HvUBI* and are shown relative to those in hexane-treated samples (grey bars). Bars represent average values of 3 biologically independent experiments +/- standard error. * = $P < 0.05$; ** = $P < 0.005$; *** = $P < 0.0005$; **** = $P < 0.0001$ (unpaired *t* test).

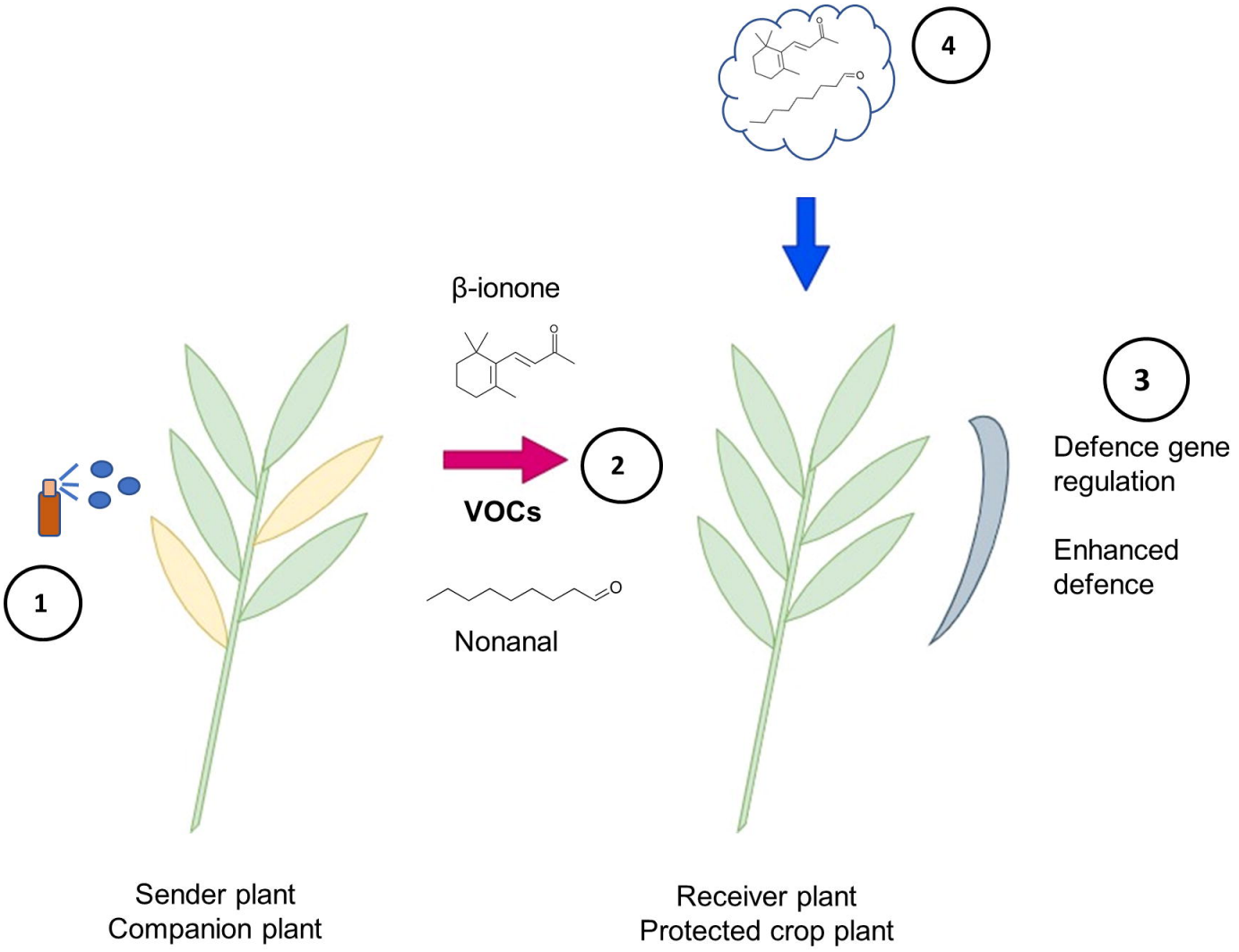

Figure 6 Working model of plant-to-plant propagation of defence in barley. After the infection with *Pseudomonas syringae* pv. *japonica* (1), barley plants emit volatile organic compounds (2) that include nonanal and β-ionone. These chemicals are recognised as defence cues in barley plants that are in the vicinity (3). Similarly, exogenous application of nonanal and β-ionone (4) induces comparable responses in barley plants that are exposed to these compounds.